

GOTOCORD

GOME Total Ozone Column Retrieval Development:

ESA ITT AO/1-4235/02/I-LG
ESRIN/Contract No. 16402/02/I-LG

WFDOAS V1.0 Delta-Validation Report

Issue 1.0

M. Weber, L.N. Lamsal, and M. Coldewey–Egbers

Institute of Environmental Physics, University of Bremen

Address:
Institute of Environmental Physics
Institute of Remote Sensing
University of Bremen FB1
P.O. Box 330 440
D-28334 Bremen
Germany

Contact:
Mark.Weber@uni-bremen.de



January 2004

Contents

1	Introduction	4
2	Relevant Documents	4
3	Reply to Reviewer's Comment	5
4	WFDOAS Comparison with TOMS V8 in 1997	13
5	WFDOAS Validation with Selected Ground-based Measurements	16
6	Discussion	29
6.1	WFDOAS validation with ground station data	29
6.2	WFDOAS Reference orbit comparison with TOMS V8	30
7	Inter-comparison of WFDOAS, TOGOMI, and GDOAS	31
8	Conclusion	36
	Appendix	37
A	GOME Reference Orbit Comparison with TOMS V8 1996-2000	37
A.1	Contour plots for GOME-TOMS V8 differences	38
A.2	Solar zenith angle dependence for GOME-TOMS V8 differences	39
B	Cosine Fitting of Satellite-Station Difference Time Series	40
C	Plots with all Stations on one Page	41
C.1	Monthly mean difference time series for WFDOAS	42
C.2	Monthly mean difference time series for GDP V3	43
C.3	Monthly mean difference time series for TOMS V8	44
C.4	Annual course of daily differences for WFDOAS	45
C.5	Annual course of daily differences for GDP V3	46
C.6	Annual course of daily differences for TOMS V8	47

C.7 Solar zenith angle dependence for WFDOAS, GDP V3, and TOMS V8 48

1 Introduction

This document serves two purposes, first, it contains a reply to the comments made by the Panel Review (see PANEL–REVIEW) and secondly it summarizes the results from the Delta Validation that was carried out after the review. The comments made by the review were fair and well balanced and the reviewers are thanked for their thoughtful suggestions. It is also agreed that all three consortia using different algorithm concepts have significantly improved total ozone retrieval as compared to the current GOME data processor version 3.0. On first sight it appears that the overall performance of all algorithms (TOGOMI, GODFIT, and WFDOAS) have produced consistent and similar results such that it was indeed hard for the review board to decide which of the algorithm is the most appropriate to succeed Version 3. Since GODFIT uses online radiative transfer calculations its processing speed is about a factor of five slower than compared to TOGOMI and WFDOAS. It was therefore decided to inter-compare TOGOMI and WFDOAS with GDOAS, a standard DOAS retrieval, that has been used by BIRA to assess the GDP V3 data quality. GDOAS closely resembles the GOME Data Processor as described in Section 6.1 in GODFIT–VALREPORT. Major differences to GDP V3 are the inclusion of the ozone filling-in like in WFDOAS, TOGOMI, and GODFIT and the use of an updated surface albedo climatology using the minimum Lambertian equivalent reflectivity database from Koelemijer et al. (2002).

The reviewers made up a list of suggestions for further validation activity to facilitate a final decision upon the new operational algorithm. Since only about one month time was given for the Delta Validation, not all the suggestions by the reviewers could be addressed and a subset of validation activities was agreed upon between the three consortia and Claus Zehner (ESA/ESRIN).

If not stated otherwise, the WFDOAS version is 1.0 as described in detail in Section 1.1, p. 4 of VALREPORT. This version uses the 326.6–335 nm spectral window. The reader should be aware that VALREPORT has been updated following the Final Presentation and the latest version should be downloaded from

www.iup.physik.uni-bremen.de/~weber/GOTOCORD/GOTOCORD_VALREPORT_V1_draft.pdf.

2 Relevant Documents

- [ATBD] WF-DOAS Algorithm Theoretical Basis Document, Issue 1.2, University of Bremen, M. Coldewey–Egbers, M. Weber, L.N. Lamsal, R. de Beek, M. Buchwitz, and J.P. Burrows, November 2003.
- [VALREPORT] WF-DOAS V1.0 Validation Report, Issue 1.2, University of Bremen, M. Weber, L.N. Lamsal, M. Coldewey-Egbers, K. Bramstedt, and K. Vanicek, January 2004.
- [PANEL–REVIEW] GOME Total Ozone Algorithm Review, ERSE-DTEX-EOPG-RP-03-0002/1, ESA/ESRIN, December 2003.
- [GODFIT–VALREPORT] The GOME Direct Fitting Validation Report, Issue 1, Revision 0, BIRA and SAO, M. van Roozendaal and R.J.D. Spurr, November 2003.
- [TOGOMI–VALREPORT] TOGOMI Product Validation Report, Issue 1.2, University of Thessaloniki and KNMI. D. Balis, P. Valks, and R. van Oss, November 2003.

3 Reply to Reviewer's Comment

Long-term Planning

In the near future a WFDOAS retrieval system with online radiative transfer modeling will be available. This approach is particularly useful for sensitivity studies with regard to wavelength selection and trace gas selection. The current version that uses look-up-tables (LUT) was specifically designed for fast retrieval without compromising the capability of full radiative transfer modeling. Our particular interest is to adapt the WFDOAS retrieval to SCIAMACHY UV/visible spectral range. As we have shown with the application of WFDOAS to SCIAMACHY near-infrared (Buchwitz et al., 2000), the WFDOAS principle is generally applicable to different instruments and spectral regions with strong (ozone, O₂, and other line absorbers) and weak atmospheric absorbers.

How does the choice of temperature impact trend monitoring?

The WFDOAS retrieval uses the temperature climatology that comes along with the TOMS V7 climatology. An ozone temperature shift correction is part of the retrieval and corrects the climatological ozone temperature (see ATBD and VALREPORT). Since we do not use meteorological analyses like ECMWF and UKMO, apparent temperature trend (real or not) in the met analyses do not play a role in WFDOAS. The influence of a real temperature trend can only enter the retrieval through corresponding trends in the spectral signature by the temperature dependence of the ozone absorption (cross-section). The comparison with the Lauder and Hohenpeissenberg time series up to March 2003 as discussed in the validation report have confirmed the long-term stability of WFDOAS as shown in Fig. 3.1. For comparison the longterm behavior of TOMS V7 overpasses for both stations are shown in Fig. 3.2. TOMS V8 overpass results (limited to period up to mid 2000) are shown for completeness in Fig. 3.3. Because of the apparent downward trend in the TOMS V7 data (after 2000), most likely due to scan mirror degradation, a correction scheme is currently in preparation to be applied to Version 8 after 2000. Similar degradation trends are observed in the GOME spectral data, but this seems not to affect the WFDOAS algorithm as demonstrated here. Except for the wavelength recalibration (done using the Fraunhofer fitting) no further adjustments in the calibration like those proposed in the GOMECAL package have been applied.

How does the choice of spectral wavelength range (start wavelength of 325 nm vs. 331 nm) impact trend monitoring?

Since our LUT covers at the moment the spectral range up to 335 nm the OMI window is currently not feasible with our retrieval. In the ATBD we have discussed the fitting window selection and we found a fit window (328.4–334.9 nm) where the ozone weighting function (wf) has minimum (absolute) correlation with temperature wf. This window is equivalent to the OMI fitting window 331–336 nm with respect to the temperature correlation (see Section 8.4 in ATBD) and this window has been tested for GOME overpasses above Lauder (mid-latitude) and Syowa (Antarctica). Not only the spectral window has been changed but also the degree of the polynomial (cubic and quadratic) that are subtracted in the differential fit. The results are shown in Fig. 3.4. Changing the polynomial

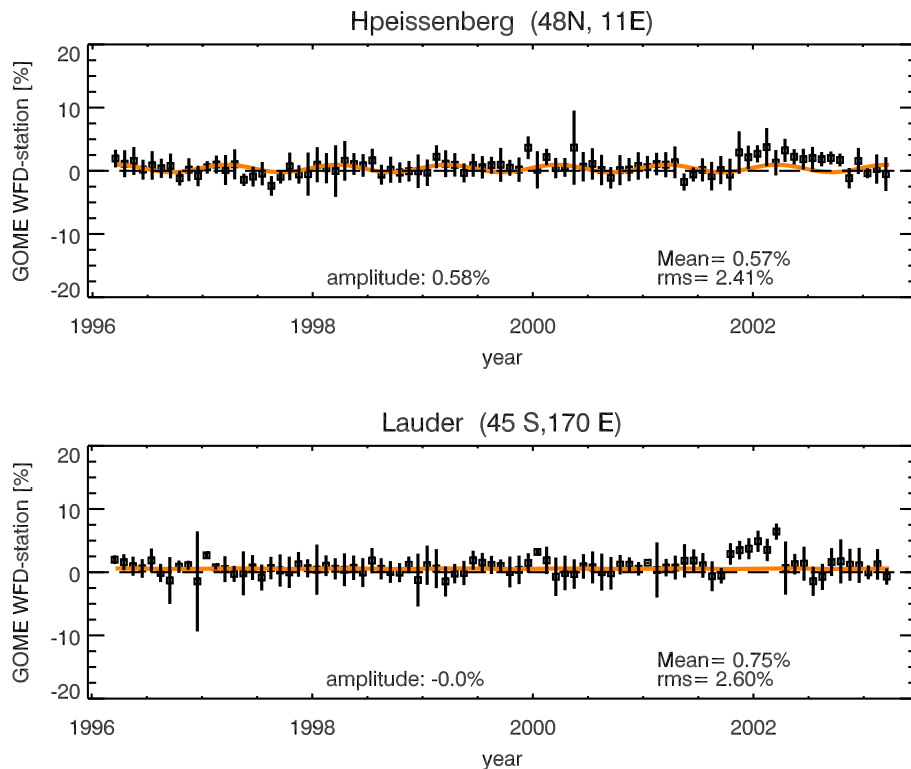


Figure 3.1: $(WFDOAS-station)/WFDOAS$ in percent for GOME overpasses over Hohenpeissenberg's Brewer (top) and Lauder Dobson instruments (collocation radius of 160 km). The error bars represents the 1σ RMS of the monthly mean and the orange line presents the fitting of a cosine time series to the daily differences. From November 2001 to October 2002 no update in the mean solar reference data were supplied in the level 1 data product and this is responsible for the larger bias during this period. The cosine fitting was limited to the period before October 2001.

degree has no effect in the larger spectral window, except for the brief period in 2002 where no update in the mean solar reference data were provided. For the smaller fit window differences of about 0.5% can be obtained if quadratic or cubic polynomials are fitted. In general it is advisable to use a smaller polynomial degree the narrower the spectral window gets. Comparing the smaller window using quadratic polynomials with V1.0, differences of up to +0.5% and a small seasonal cycle variation with amplitudes close to 0.3% is noted. This indicates that spectral window and polynomial degree selection in the DOAS fitting can alter results to within a half percent and also slightly modify the seasonal cycle variation when compared with ground data. Selection of fitting window and polynomial may also play a larger role when (differential) degradation effects become larger as seen in the brief period in 2002. The extraction of proper mean solar spectra from the individual solar spectra recorded during the daily solar scan is currently in preparation and shall alleviate the problems currently observed in 2002.

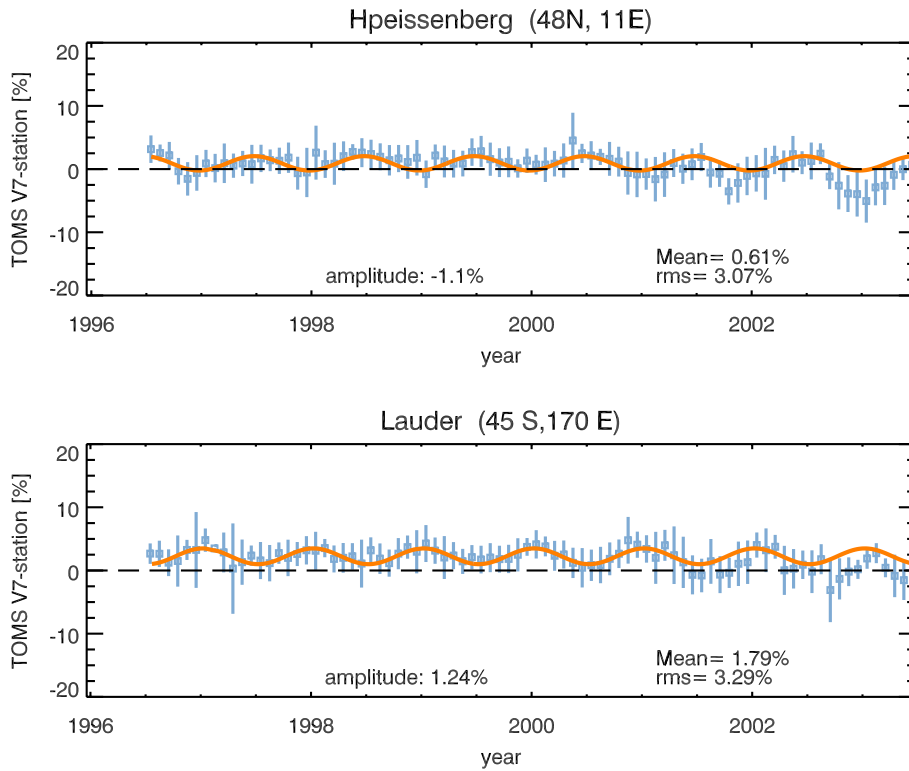


Figure 3.2: Same as Figure 3.1 but for TOMS V7 overpasses above Hohenpeissenberg (top) and Lauder (bottom). Here collocation radius was 100 km and the cosine fitting (orange line) was again limited to the period before October 2001.

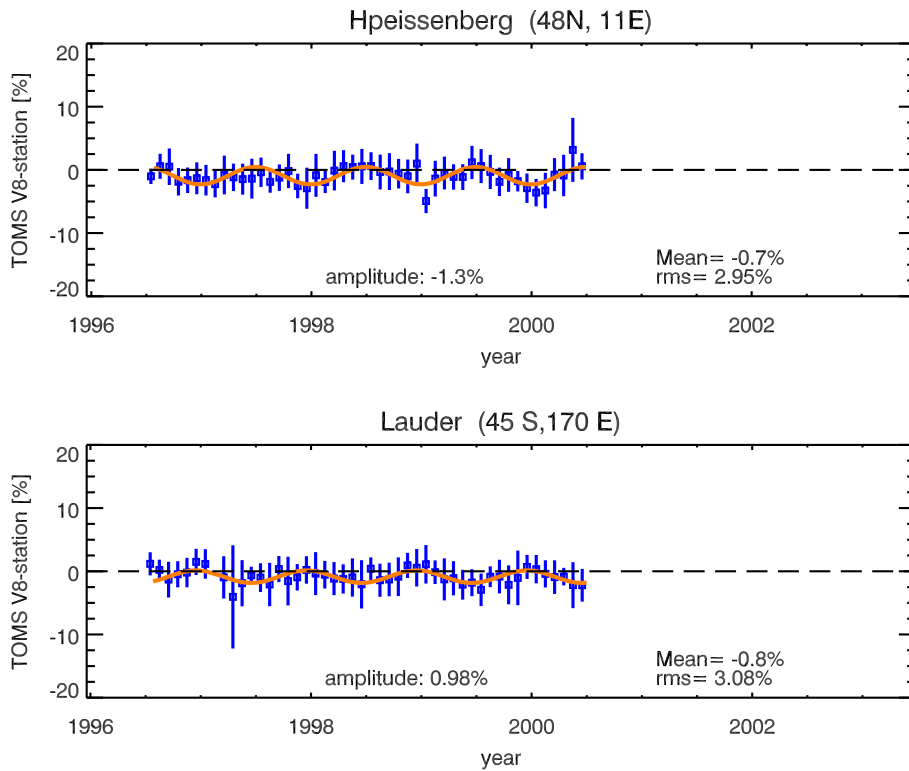


Figure 3.3: Same as Figure 3.2 but shown for TOMS V8 overpasses above Hohenpeissenberg (top) and Lauder (bottom) up to June 2000.

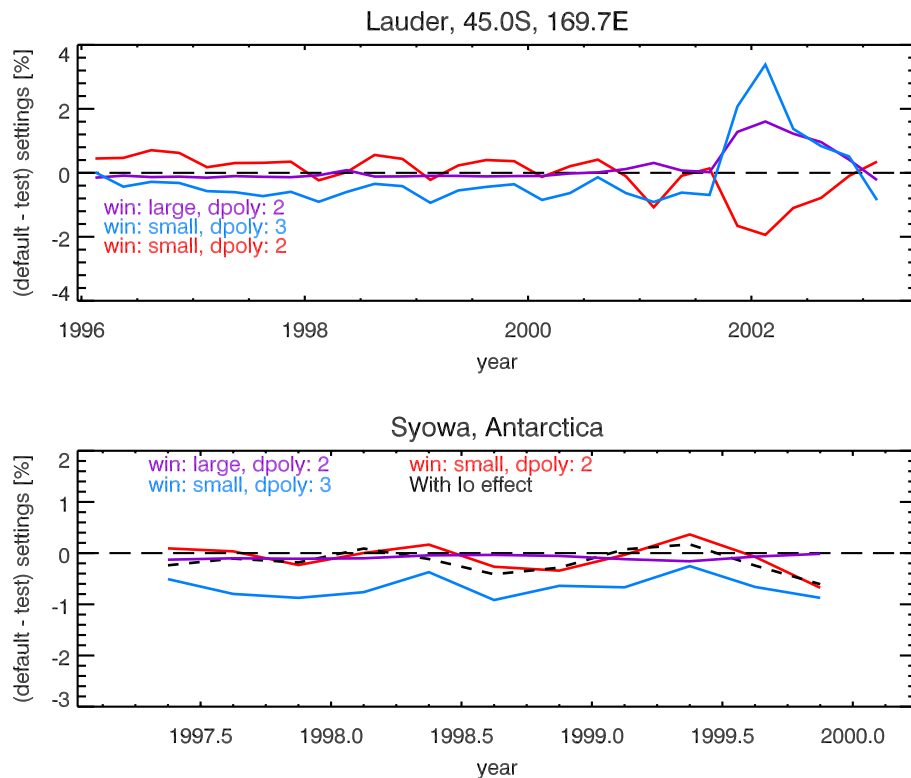


Figure 3.4: Difference to WFDOAS Version 1.0 (326.6–335 nm and cubic polynomial) for GOME overpasses over Lauder (top) and Syowa (bottom). Pink: 326.6–335 nm and quadratic polynomial. blue: 328.4–334.9 nm and cubic polynomial, red: same as blue but quadratic polynomial, black dash: same as red but including I_o -effect (only Syowa).

How does the ozone profile information impact the total ozone? How does TOMS V7/V8 total ozone dependent climatology impact the total column?

For testing the new V8 climatology new LUT have to be generated and this is not feasible in the short time left for the Delta Validation (until end of January). The comparison of the GOME reference orbit WFDOAS results from 1997 with the gridded level 3 TOMS V8 data show similar features in the differences as the TOGOMI results (see viewgraphs from the Final Presentation) that uses the TOMS V8 climatology. From this it can be concluded that the use of TOMS V7 and TOMS V8 profile climatology apparently yield quite similar results. A more detailed discussion can be found in Sections 4 and 7.

In the validation report we have used different climate zones in the profile shape climatology for the WOUDC station data. Mid-latitude and high-latitude stations were analyzed each with both high-latitude and mid-latitude TOMS V7 profiles. In general the proper climate zone profiles provided the best results. The error from a false climate zone profile can be a few percent for a given orbit as discussed in the ATBD (see Section 6 in ATBD, p. 29ff).

Are there systematic differences between the three GOME ground-pixels?

This is indeed a good point that has not been addressed for any of the algorithms presented during the Final Presentation. Figure 3.5 shows the time series separated by scan pixel type (0: East, 1: Nadir, 2: West) for ten of the ground-based stations selected for the Delta Validation. No statistically significant tendency is recognizable, but for selected stations differences between pixel types results can reach 0.5%. It should be noted here that for the differences observed at a given day only one of the three pixel types are plotted, whichever was the closest in distance to the station. That may cause different sampling sizes for the various pixel types and may explain the apparent differences at selected stations, particularly in the polar region. For reference the scan angle dependent time series are also shown for GDP V3 in Fig. 3.6.

Ground stations in deserts should be included in the validation set

Desert stations are of interest here because of the elevated surface albedo and enhanced absorbing aerosols (mineral dust) in this region. A warning should be placed here that station data from this region may not be reliable. However a consistency check between the three algorithms in this region may be more reasonable but is not planned as part of the Delta Validation. Comparison between all three algorithms in general is presented in Section 7 of this report.

Inter-comparison to the new TOMS V8 shall be performed

The TOMS V8 Version has not been officially released yet and is currently being validated by the NASA group. Such a comparison can not be regarded as a validation, but is nevertheless helpful for investigating the global and seasonal distribution of the differences between TOMS V8 and the new GOME algorithms. As part of the Delta Validation 467 GOME orbits (roughly one orbit per day) from the reference orbit set covering 1997 will be analyzed and compared with the gridded TOMS V8 data provided by NASA (see Section 4 of this report).

How does different calibration (e.g. wavelength and polarization) impact the algorithm?

We have introduced in WFDOAS the so-called Fraunhofer fit that makes the inversion independent of the wavelength calibration with the lamp line source and in addition automatically corrects for the Doppler shift in the solar spectrum due to the orbital motion of ERS-2. As wavelength reference for the GOME solar spectra serves the high resolution solar atlas from Kurucz et al. (see ATBD) after convolution with the proper GOME slit function. Without the Fraunhofer fit the total ozone gets smaller by about 2% (see ATBD).

Atmospheric polarization is not corrected for in the radiative transfer calculation and the scan pixel dependence can shed light into that issue. However, it was found that there are no systematic differences between the ground pixel types.

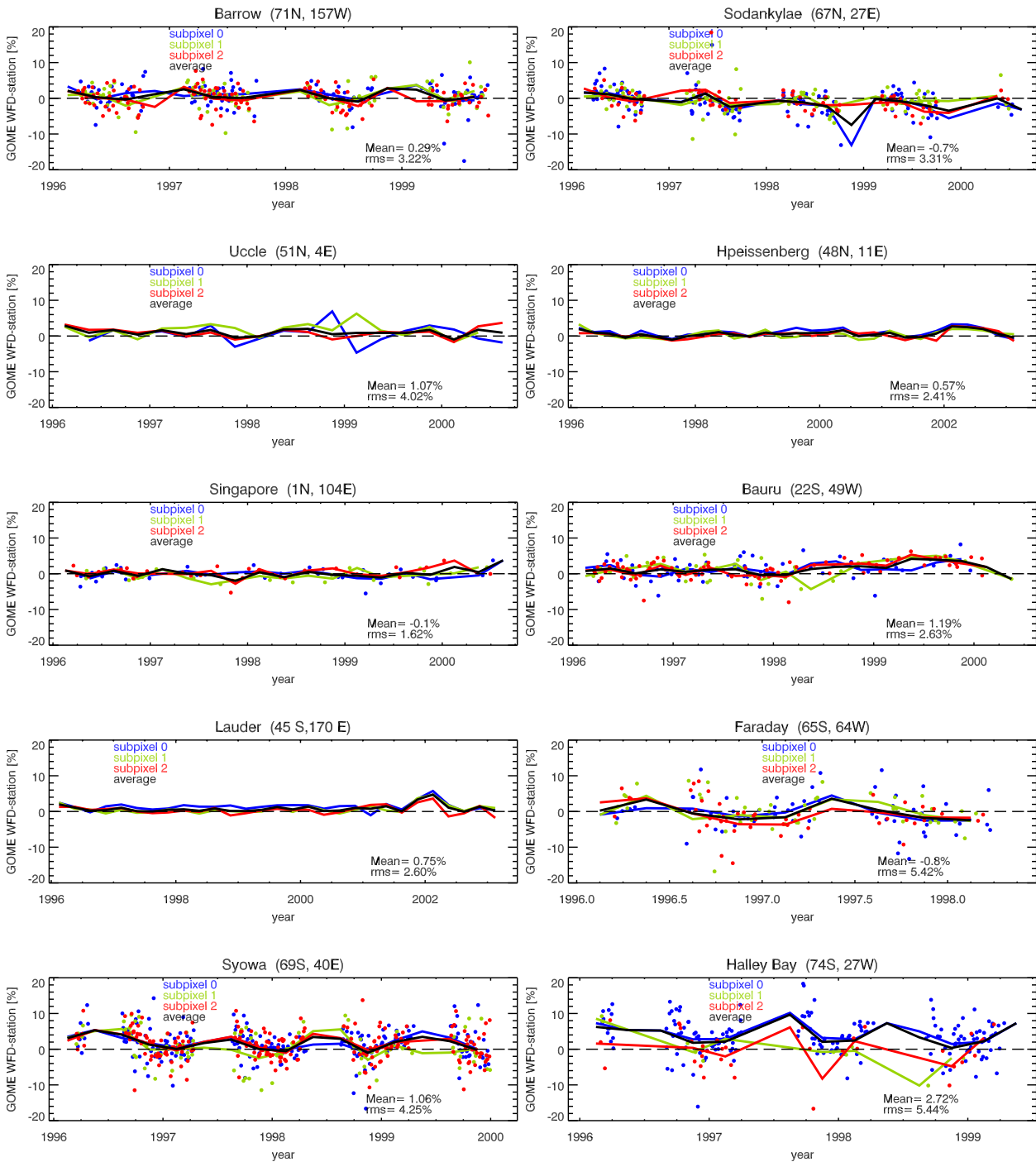


Figure 3.5: Scan angle dependence of $(WFDOAS-station)/WFDOAS$ in percent for GOME overpasses over selected ground stations. For all stations daily differences are also plotted except for Uccle, Hohenpeissenberg, and Lauder, where only the three month means are shown. At a given day only the nearest GOME overpass was selected that either belonged to East (subpixel 0, blue), Nadir (subpixel 1, green), or West pixel (subpixel 2, red).

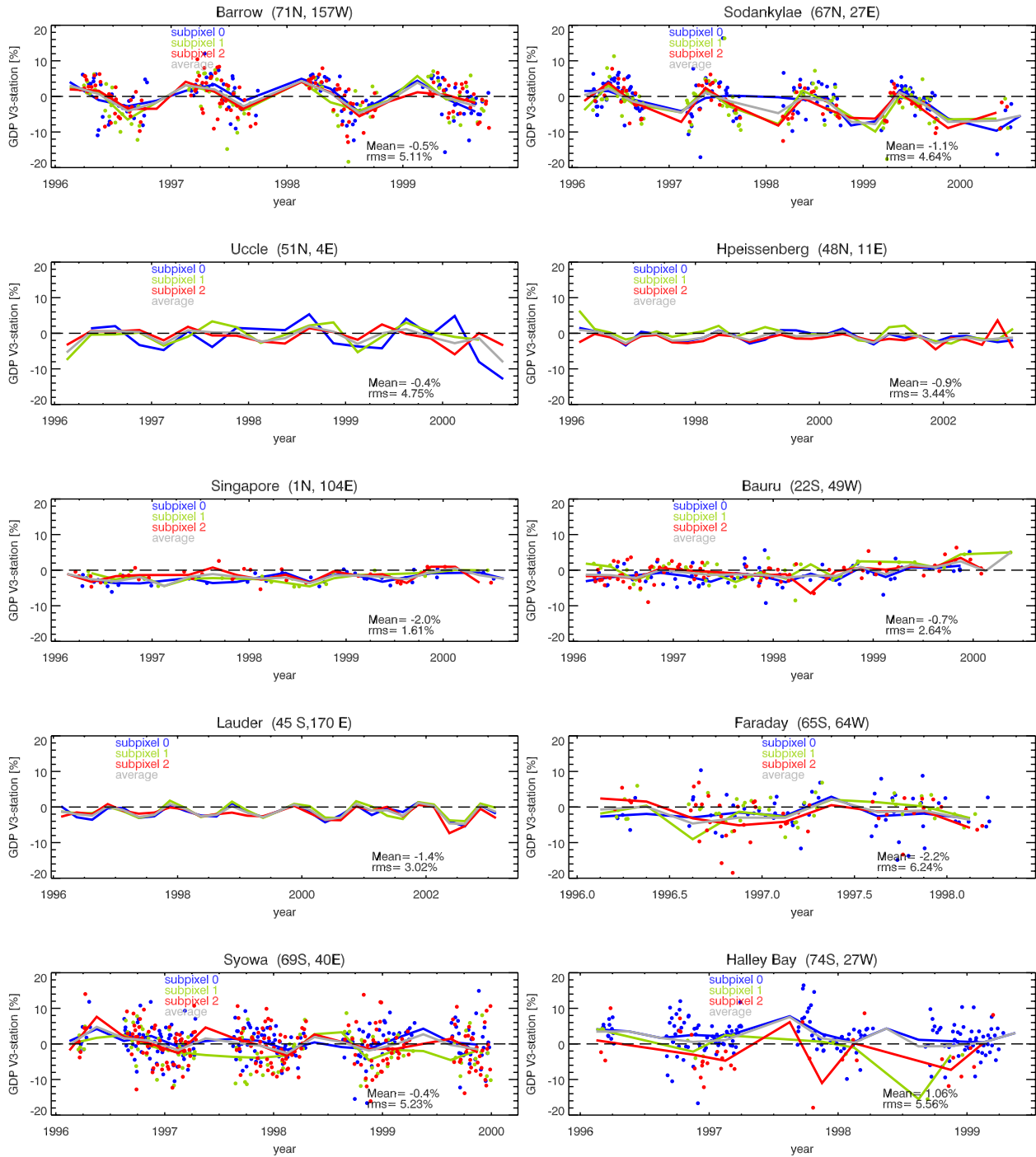


Figure 3.6: Same as Fig. 3.5 but for GDP V3.

Other potential error sources come from the polarization correction algorithm that corrects for instrumental polarization effects. As part of the GOME-2 error study (see ATBD) that error was quantified and estimated not to exceed 0.3%.

The review panel has recommended to use the GOMEAL algorithm for the generation of GOME level 1 products (calibrated radiance and irradiance spectra). This has not been used in the WFDOAS algorithm and the validation results indicate no need to use the additional calibration correction provided by GOMEAL. Since the three new GOME algorithms have produced consistent results although some of them use GOMEAL and others not, this recommendation is in our opinion not well justified.

How do aerosols impact the algorithm?

A detailed aerosol investigation has been reported in the ATBD document. The effective albedo formulation in WFDOAS represents a first order aerosol correction. Using simulated data it was shown that for non-absorbing aerosols with extremely high optical aerosol depth (3-5) the errors were well below 0.5%. For absorbing aerosols (stratospheric volcanic and tropospheric) the errors can be up to a few percent (see Section 7, Table 7.1, p. 34 in ATBD). Generally, non-absorbing aerosols leads to an underestimation of the ozone column. For volcanic aerosols (mainly stratospheric) an error of -1% can be expected at an aerosol optical depth of 0.6 and single scattering albedo of 0.81.

Self-consistency checks

An agreement between the consortia and Claus Zehner on the extent of the Delta Validation activities in January 2004 was agreed upon. It includes a comparison to TOMS V8 for the 1997 reference orbits and eleven selected ground stations using different type of measurements from Brewer (Sodankylae, Hohenpeissenberg, and Uccle), Dobson (Barrow, Singapore, Lauder, Faraday, Syowa, and Halley Bay) and UV/vis DOAS type spectrometers (Bauru and Rothera) covering all regions from pole to pole. Using the same graphical presentation of the data sets permits a more direct comparison of the three algorithms. The WFDOAS comparison with TOMS V8 is summarized in Section 4 and validation with selected ground stations are summarized in Section 5 and discussed in Section 6. Inter-comparison between WFDOAS, TOGOMI, and GDOAS using the 1997 reference orbits are presented and summarized in Section 7.

4 WFDOAS Comparison with TOMS V8 in 1997

The methodology of comparison with the gridded $1^\circ \times 1.25^\circ$ TOMS V8 data, as kindly provided by NASA prior to their official release, has been described in the TOGOMI-VALREPORT (Section 4.2.2, p. 20–21). For each GOME pixel analyzed the closest grid value for TOMS from the same day was selected and the difference taken. In the top panel of Fig. 4.1 the monthly mean difference in 1° latitude steps are shown as derived from the GOME reference orbits. Only GOME data from the normal forward scan mode (960 km swath width with East, Nadir, and West pixels) have been used here. Since there are about one reference orbit per day, the longitudinal sampling is very limited, but nevertheless, a reasonable sampling of the seasonal variability for each latitude is achieved.

At low and middle latitudes WFDOAS is about 0-2% higher than TOMS V8. A weak seasonal cycle is visible in the differences with maxima in winter and minima in summer. These variations are usually below 0.5%. Larger positive differences exceeding in some cases 5% are observed at high latitudes and high solar zenith angles, particularly during late winter/early spring.

A comparison between WFDOAS and GDP V3 is shown in the bottom panel of the same figure. Larger differences are observed in the comparison with GDP Version 3.0 with differences ranging between 0 and 4%. The solar zenith angle dependence of the differences is shown in Fig. 4.2. A hemispheric bias is apparent in the WFDOAS-TOMSV8 differences for intermediate solar zenith angles. That points at the problem with the TOMS algorithm (Bramstedt et al., 2003) that to a larger extent was apparent in TOMS V7, but seems to be still prevalent but much reduced in the new TOMS Version. Between WFDOAS and GDP V3 the solar zenith angle dependent differences are similar for both hemispheres and the differences increases towards 80° (+3%) and decreases again beyond that point.

A summary plots for the period 1996 to 2000 is shown in Appendix A. The basic features observed here remain valid for the extended period. Further discussion of these results can be found in the Discussion section (Section 6).

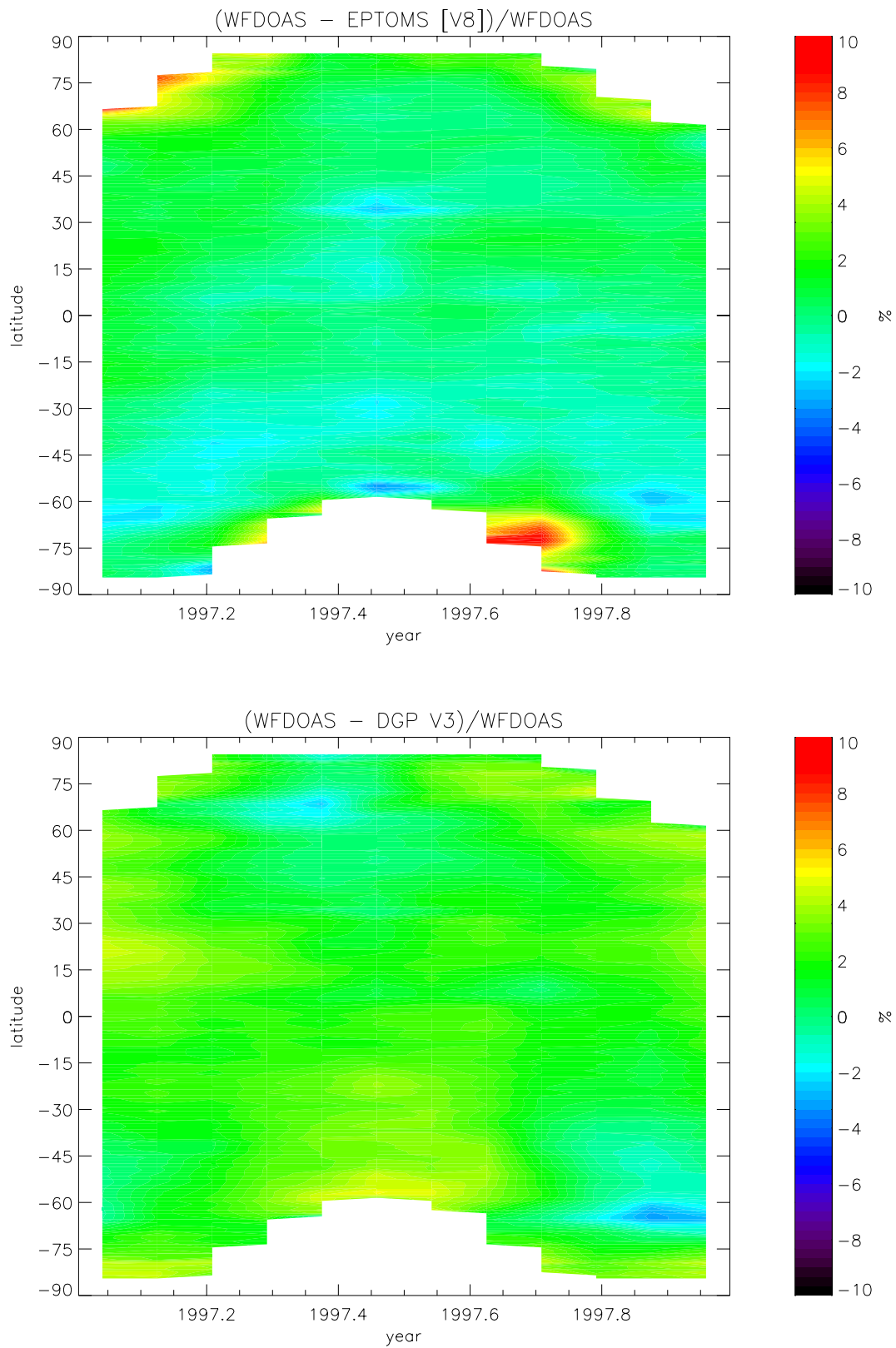


Figure 4.1: Monthly mean differences between WFDOAS and daily gridded TOMS V8 data (top) and between WFDOAS and GDP V3 (bottom) for the GOME reference orbit dataset in 1997.

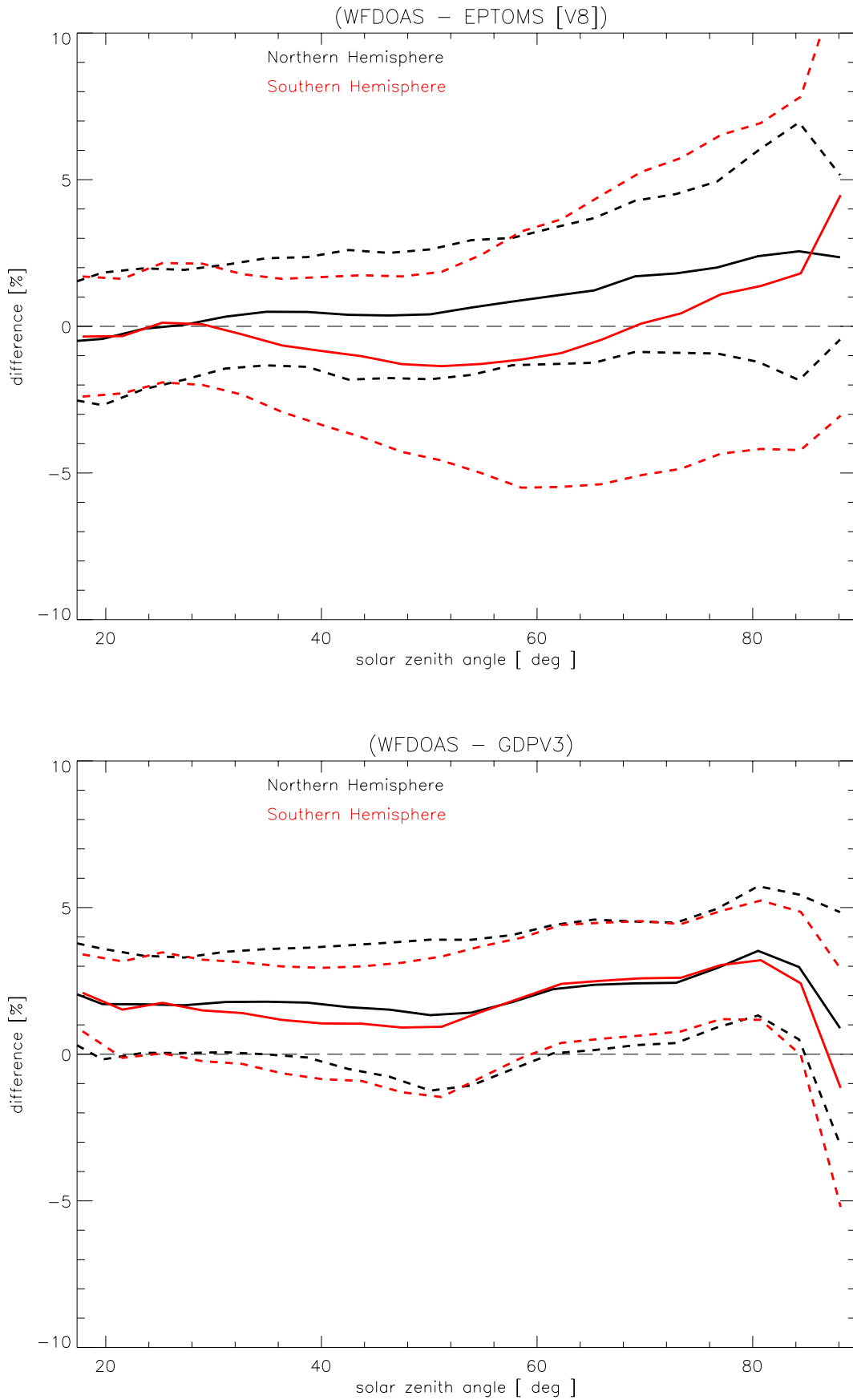


Figure 4.2: Solar zenith angle dependence of the WFDOAS-TOMSV8 (top) and WFDOAS-GDPV3 (bottom) monthly differences as shown in Fig. 4.1. Dashed lines are the 1σ RMS from averaging individual matches from the reference orbit data set.

5 WFDOAS Validation with Selected Ground-based Measurements

A list of eleven stations with different instrumentations (Brewer, Dobson, and UV/Vis DOAS spectrometers) has been selected for the Delta Validation exercise. In Table 5.1 all stations and their locations are summarized. UV/vis instruments, mainly from the SAOZ network, have been selected to investigate the solar zenith angle dependence that may differ from other instruments particularly at high solar zenith angles (Brewer and Dobson). For each station the closest overpass to within a maximum collocation radius was selected. For Hohenpeissenberg and Lauder the maximum allowable radius was 160 km, while for other stations 300 km was chosen. Using overpass tables for TOMS V8 (provided by NASA), a matching TOMS V8 value for each matched pair of GOME and station data was extracted. Only for Hohenpeissenberg and Lauder, all overpasses from TOMS are used irrespective of matches with GOME. Maximum collocation radius for TOMS was set to 100 km as provided in the NASA overpass tables.

Table 5.1. List of station data used in the Delta Validation.

Station No.	Instrument	Latitude	Longitude	Altitude [m]	Location
199	Dobs	71° N	157° W	11	Barrow/Alaska, USA
262	Brew	64° N	27° E	179	Sodankylae, Finland
053	Brew	51° N	4° E	100	Uccle, Belgium
099	Brew	48° N	11° E	975	Hohenpeissenberg, Germany
214	Dobs	1° N	104° E	14	Singapore, Singapore
614	Saoz	22° S	49° W	522	Bauru, Brazil
256	Dobs	45° S	170° E	370	Lauder, New Zealand
017	Dobs	65° S	64° W	10	Faraday, Antarctica
709	Saoz	68° S	68° W	0	Rothera, Antarctica
101	Dobs	69° S	40° E	21	Syowa, Antarctica
057	Dobs	74° S	27° W	31	Halley Bay, Antarctica

Figures 5.1-5.11 show the satellite comparison with the collocated ground-based measurements for all stations listed in Table 5.1. The differences as shown in these plots are defined as follows

$$\Delta = (\text{satellite} - \text{groundbased})/\text{satellite},$$

and are plotted in different ways. To the left are monthly mean differences for WFDOAS, GDP V3, and TOMS V8 as a time series (from top to bottom). To the right the same is shown for the individual overpasses but as a function of the day within a year. The larger panel at the bottom shows the solar zenith angle dependence of the differences. The orange solid line is the result from a cosine fit with a period of 366 days to the daily differences. From this fit an annual mean (A), wave amplitude (B), and phase (ϕ) can be derived (see section 7.2.2 in GODFIT-VALREPORT). Further details of this fitting is given in Appendix B. In Appendix C the various type of plots have been regrouped for each type of plot with all stations on one page.

The annual mean differences stated in the plots are from the daily difference averaging. The RMS indicates the 1σ scatter of the daily differences. The spatial resolution (higher for TOMS) and the collocation radius setting may have an influence on the RMS scatter. However, the scatter for GDP

V3 can be directly compared with WF DOAS and are generally higher for the former confirming the improved quality through the WFDOAS retrieval.

Tables 5.2 and 5.3 summarizes the cosine fit results. For some polar stations the annual mean from the cosine fitting is significantly different from the mean calculated from the daily difference values. This is due to the absence of polar night data. For this reason the annual mean are presented in two different ways.

The results from this comparison with selected ground stations and TOMS V8 as shown in the previous sections are summarized and discussed in the next Section.

Table 5.2. Mean difference to station from cosine fitting to time series (A) and from averaging daily differences.

Loc.	Instr.	Lat.	Mean difference (cosine fit)			Mean difference (daily)		
			[%]			[%]		
			WFDOAS	GDP V3	TOMS V8	WFDOAS	GDP V3	TOMS V8
Barr	Dobs	71° N	1.2	0.3	-0.4	0.3	-0.5	-0.1
Soda	Brew	64° N	-1.2	-4.2	-3.0	-0.7	-1.1	-2.1
Uccl	Brew	51° N	1.0	-0.6	0.1	1.1	-0.5	0.2
Hohe	Brew	48° N	0.4	-0.9	-0.9	0.6	-0.9	-0.8
Sing	Dobs	1° N	-0.2	-2.0	0.7	-0.1	-2.0	0.7
Baur	Saoz	22° S	1.2	-0.8	2.3	1.2	-0.8	2.3
Laud	Dobs	45° S	0.6	-1.3	-0.9	0.8	-1.4	-0.9
Fara	Dobs	65° S	-0.1	-2.1	-1.5	-0.8	-2.2	-1.3
Roth	Saoz	68° S	4.2	3.6	0.4	4.5	4.6	2.4
Syow	Dobs	69° S	2.3	0.4	-0.5	1.0	-0.4	-0.3
Hall	Dobs	74° S	5.1	2.9	4.0	2.7	1.1	2.4

Table 5.3. Amplitude (B) and phase (ϕ) from cosine fitting to time series of satellite-station difference.

Loc.	Instr.	Lat.	Amplitude			Phase		
			[%]			[days]		
			WFDOAS	GDP V3	TOMS V8	WFDOAS	GDP V3	TOMS V8
Barr	Dobs	71° N	1.9	4.3	-1.0	11	54	-56
Soda	Brew	64° N	-1.6	-5.7	-2.0	-66	-14	4
Uccl	Brew	51° N	-0.7	-1.9	-2.1	-17	58	-6
Hohe	Brew	48° N	0.6	-1.5	-1.4	80	-65	-3
Sing	Dobs	1° N	-0.3	0.7	0.7	57	1	-73
Baur	Saoz	22° S	-0.5	0.5	-0.3	12	-27	9
Laud	Dobs	45° S	-0.0	1.7	1.0	-73	-25	-16
Fara	Dobs	65° S	-2.9	0.8	3.3	-27	86	42
Roth	Saoz	68° S	1.3	3.8	7.1	-23	-9	-12
Syow	Dobs	69° S	-3.1	-2.2	1.3	-7	-3	41
Hall	Dobs	74° S	-4.9	-3.7	-3.3	-6	-5	-25

Barrow, Alaska, USA, 71°N, Dobson

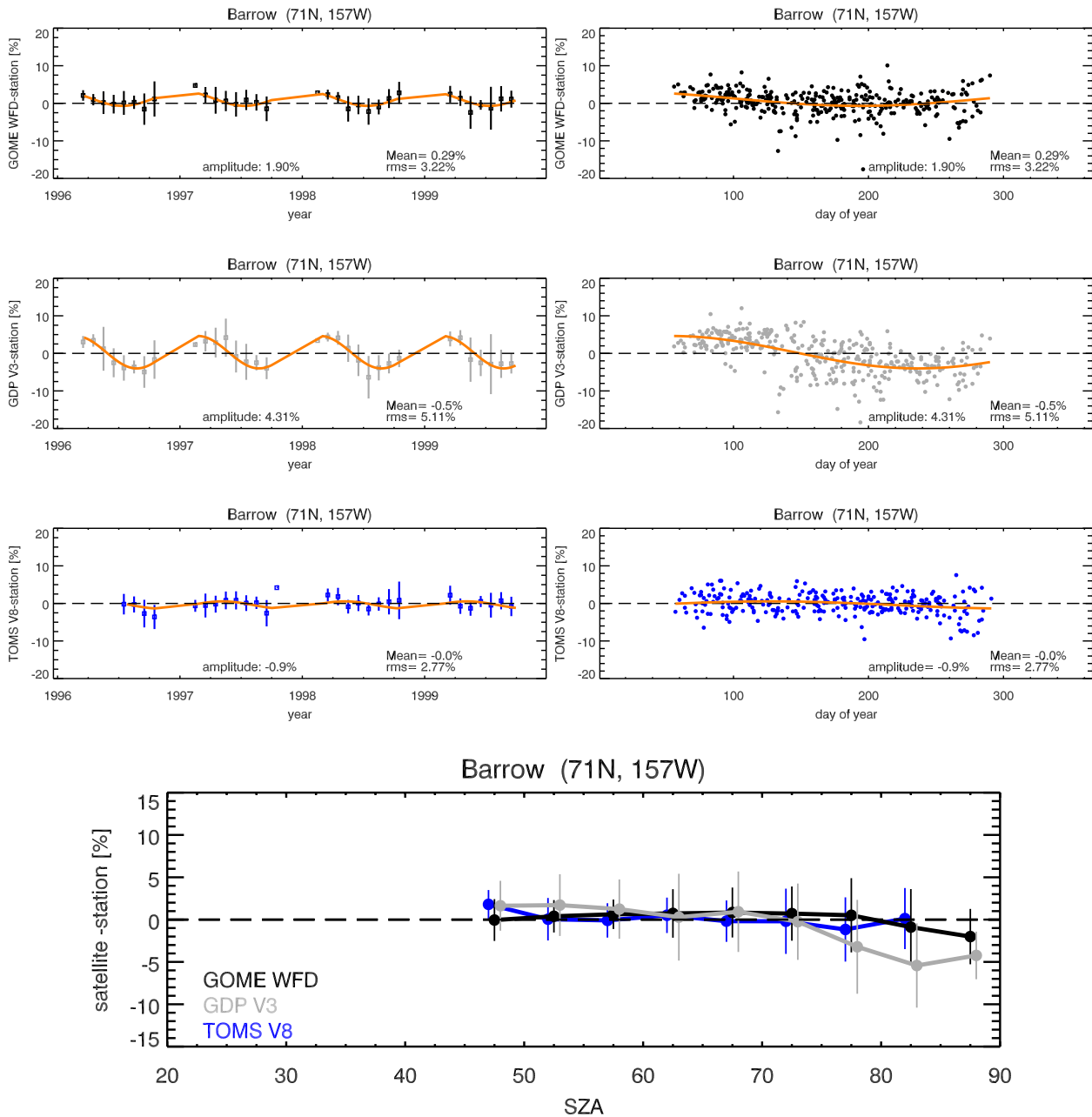


Figure 5.1: Left: Barrow, Alaska (71°N). Left: monthly mean difference between satellite and ground based data for WFD (black), GDP V3 (light grey), and TOMS V8 (blue). Right: daily differences as a function of the day within a year for WFD (black), GDP V3 (light grey), and TOMS V8 (blue). Bottom: Solar zenith angle dependence of the differences for WFD, GDP V3, and TOMS V8. Orange line represents the cosine fitting to the time series using the daily values (see Appendix B for details).

Sodankylae, Finland, 64°N, Brewer

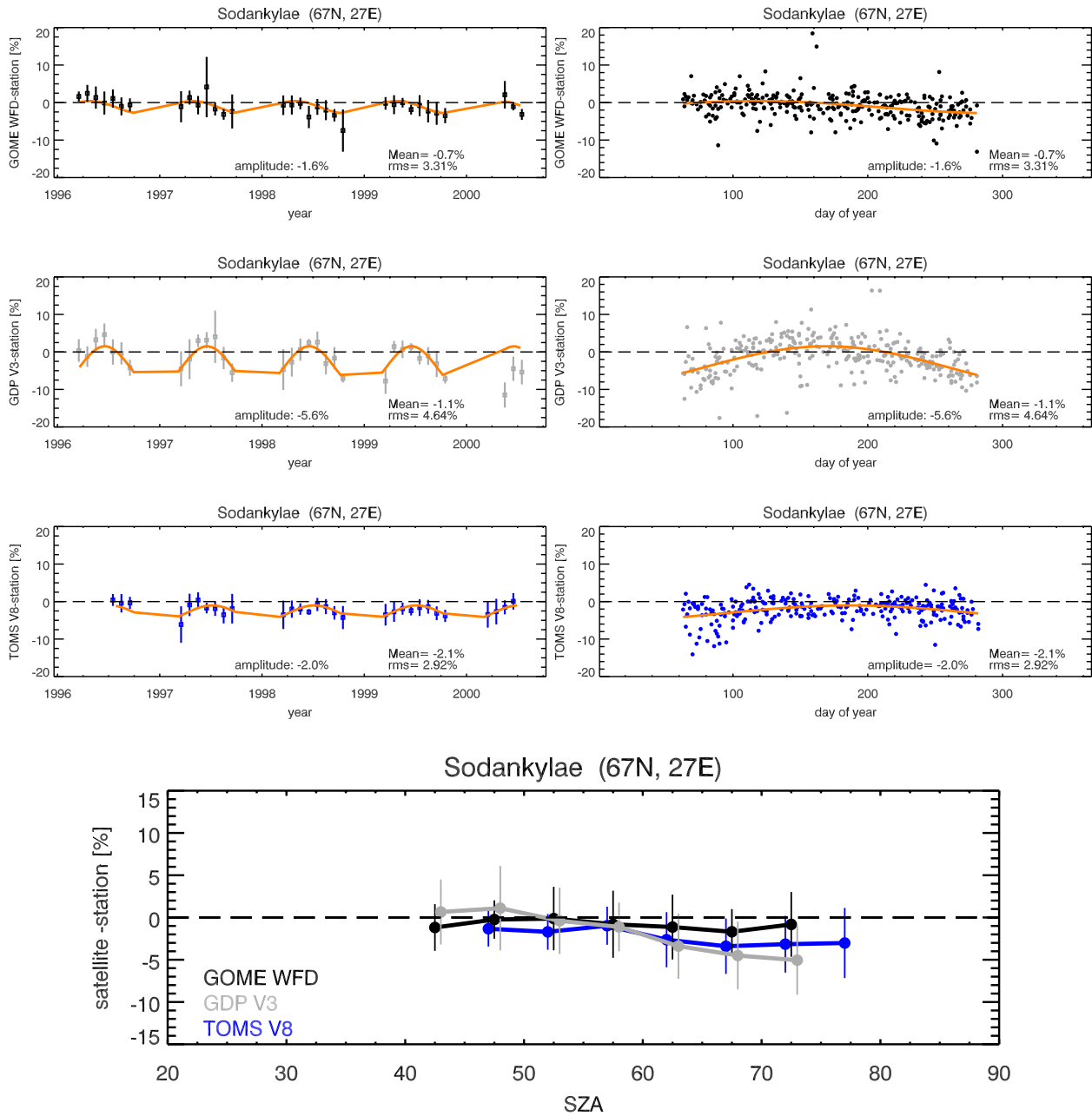


Figure 5.2: Same as Fig. 5.1 but for Sodankylae, Finland, 64°N

Uccle, Belgium, 51°N, Brewer

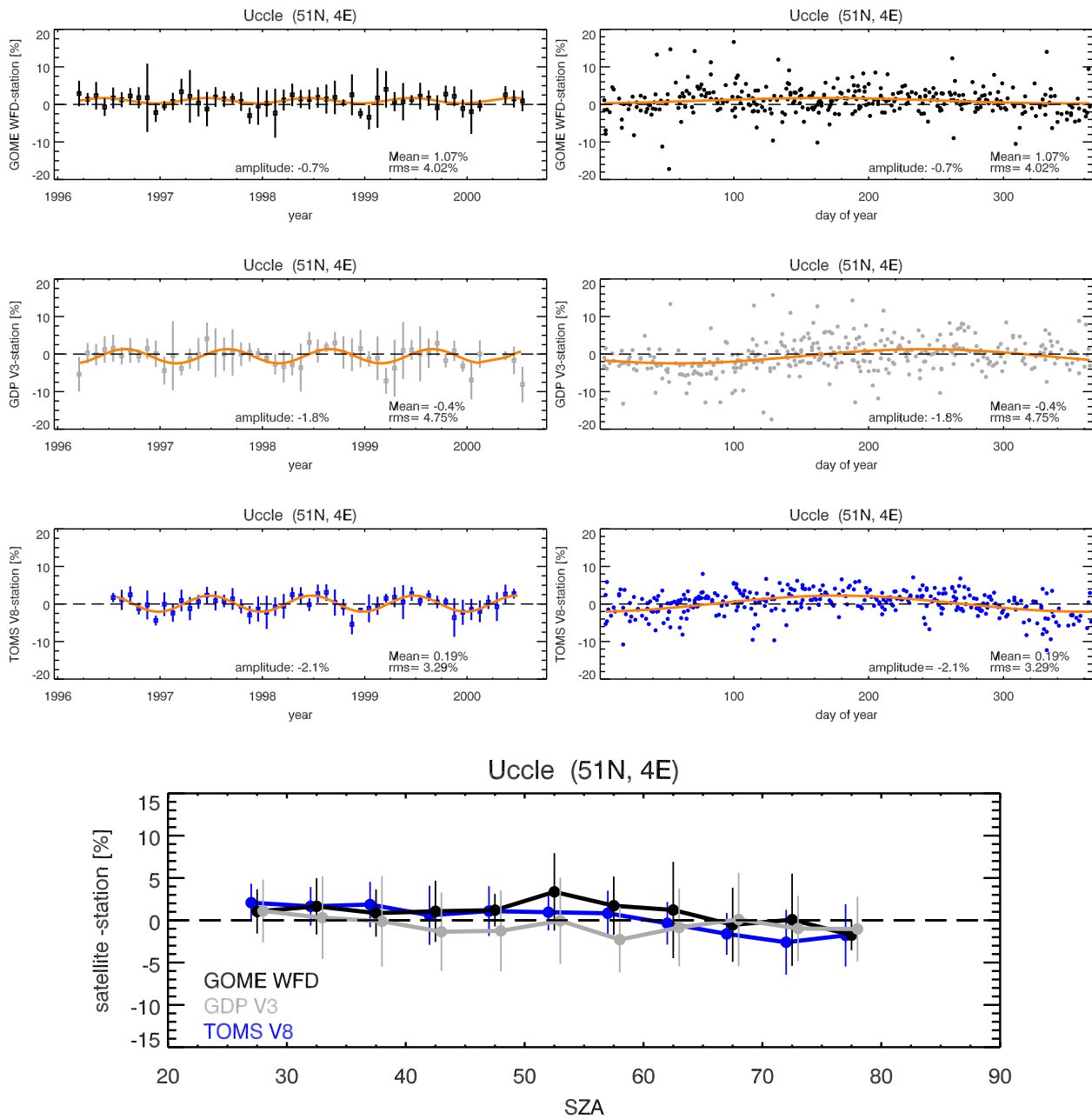


Figure 5.3: Same as Fig. 5.1 but for Uccle, Belgium, 51°N

Hohenpeissenberg, Germany, 48°N, Brewer

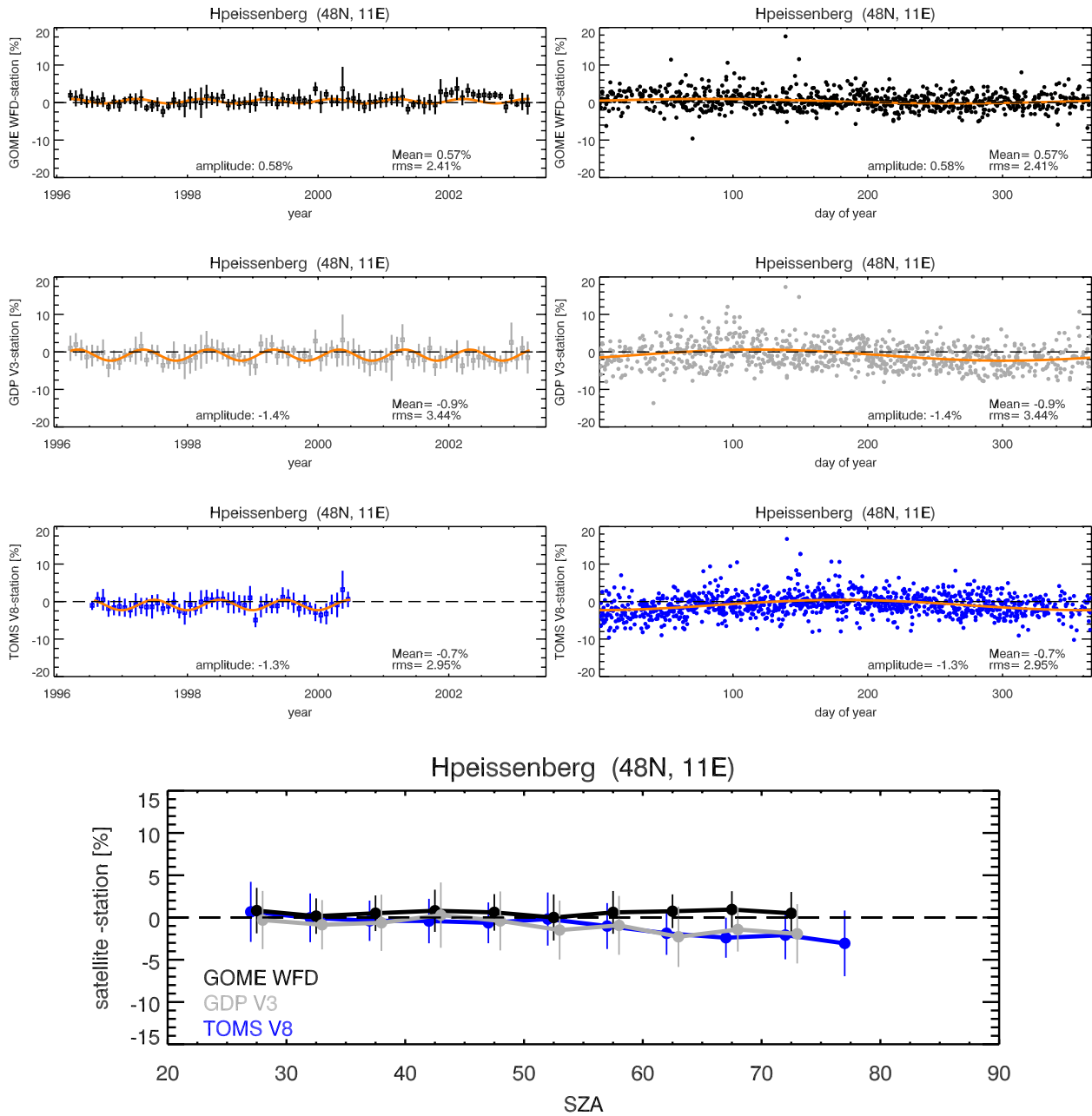


Figure 5.4: Same as Fig. 5.1 but for Hohenpeissenberg, Germany, 48°N.

Singapore, 1°N, Dobson

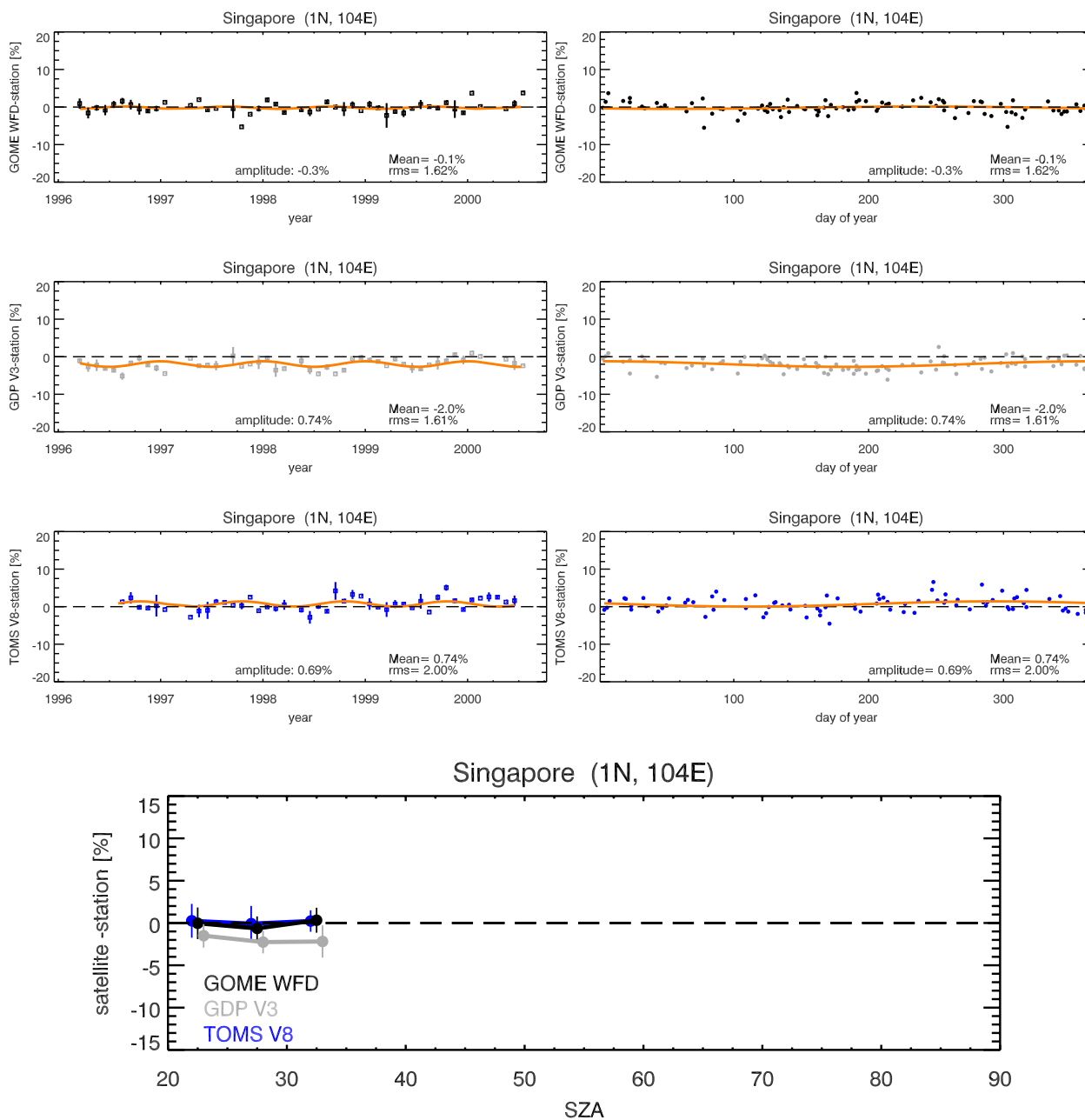


Figure 5.5: Same as Fig. 5.1 but for Singapore, 1°N.

Bauru, Brasil, 22°S, SAOZ

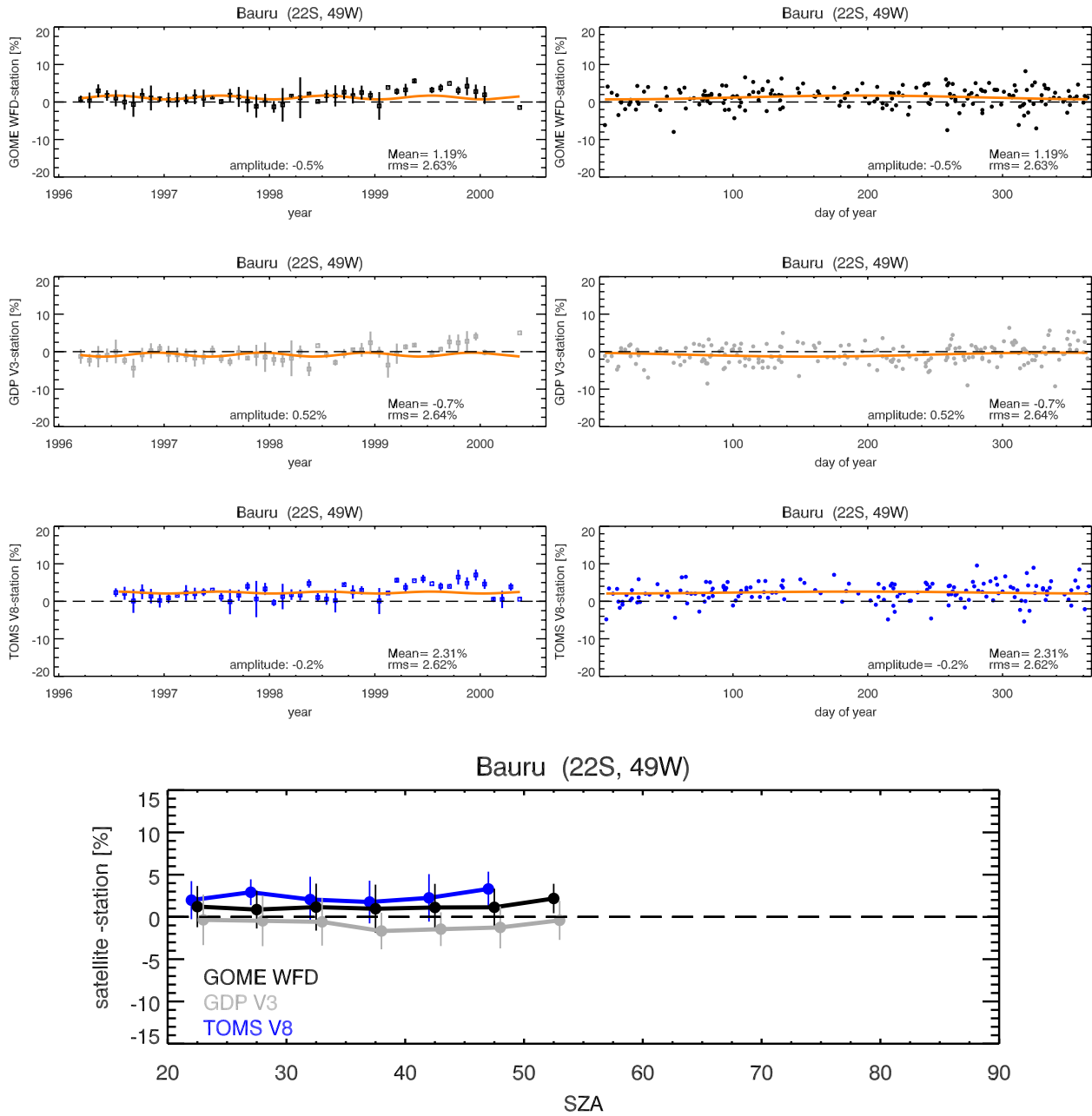


Figure 5.6: Same as Fig. 5.1 but for Bauru, Brasil, 22°S.

Lauder, New Zealand, 45°S, Dobson

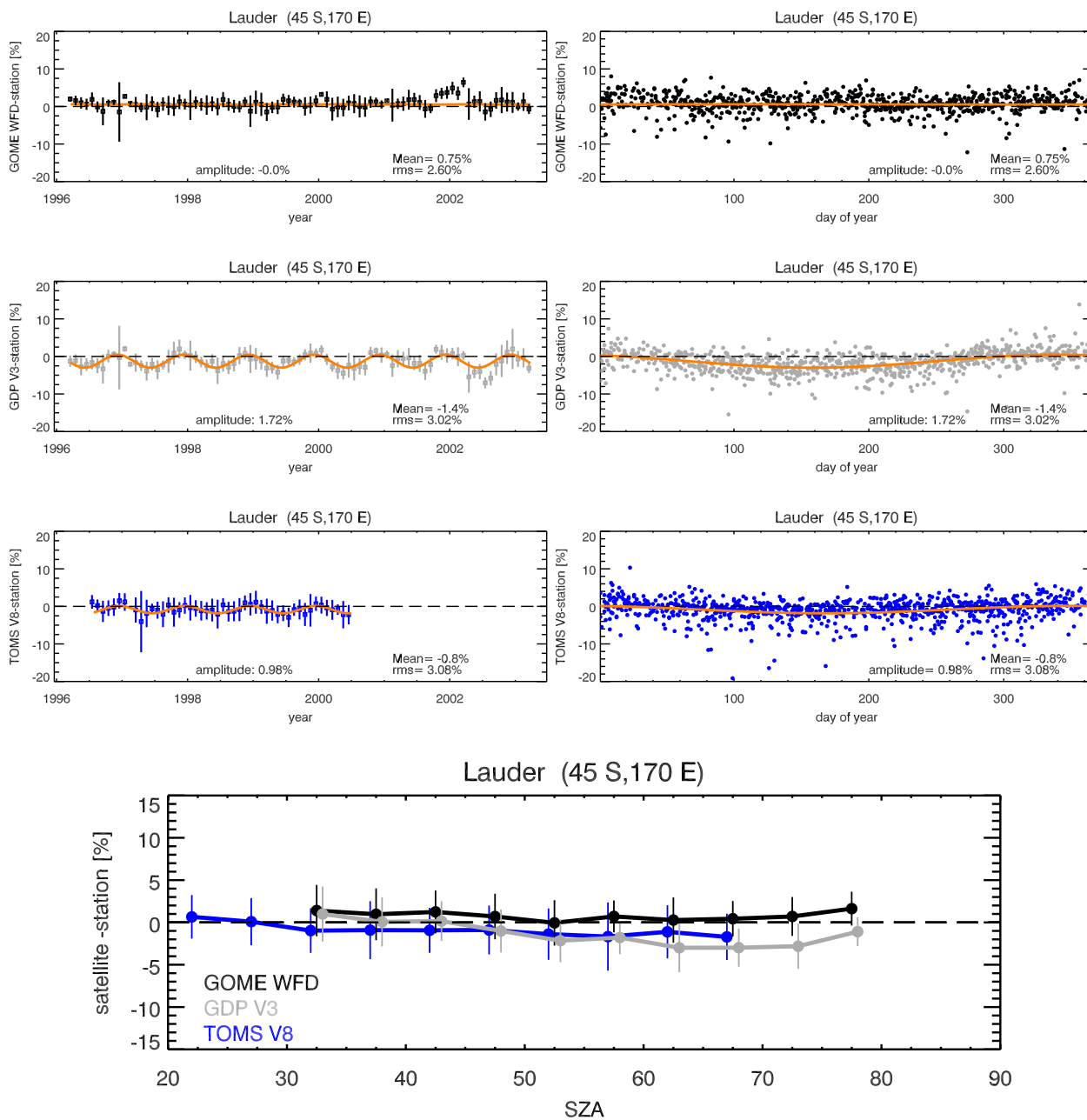


Figure 5.7: Same as Fig. 5.1 but for Lauder, New Zealand, 45°S.

Faraday, Antarctica, 65°S, Dobson

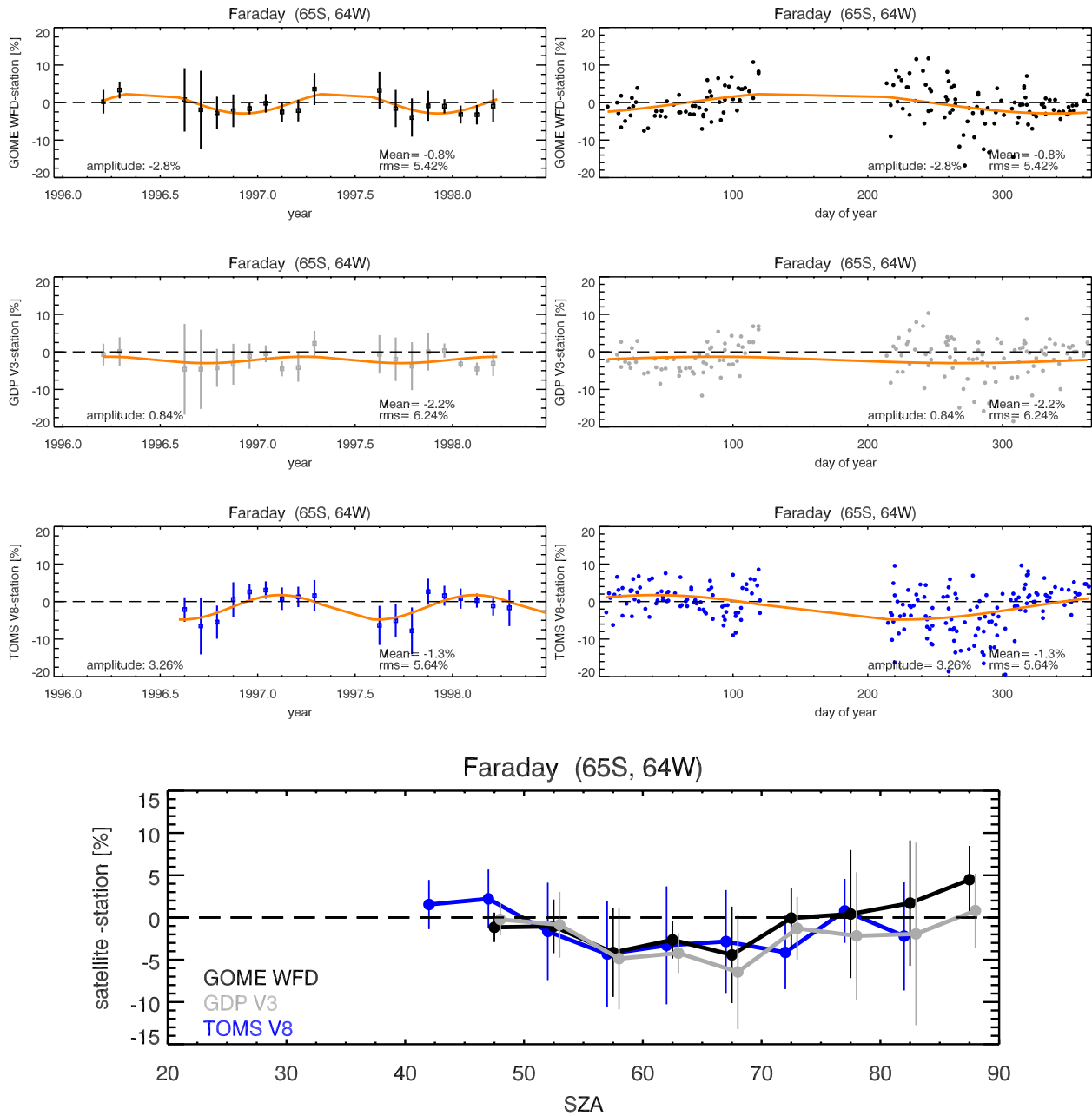


Figure 5.8: Same as Fig. 5.1 but for Faraday, Antarctica, 65°S.

Rothera, Antarctica, 68°S, SAOZ

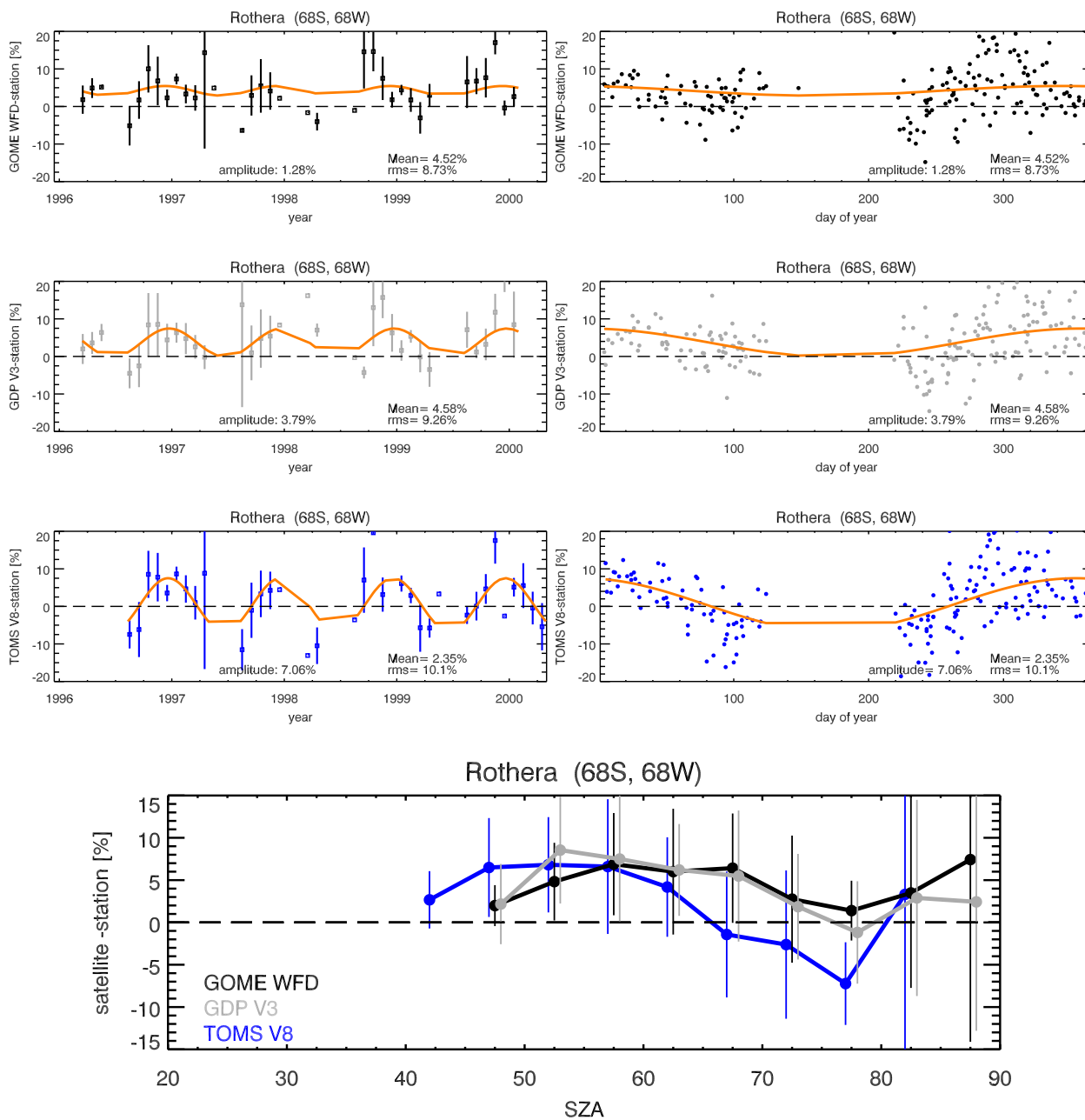


Figure 5.9: Same as Fig. 5.1 but for Rothera, Antarctica, 68°S.

Syowa, Antarctica, 69°S, Dobson

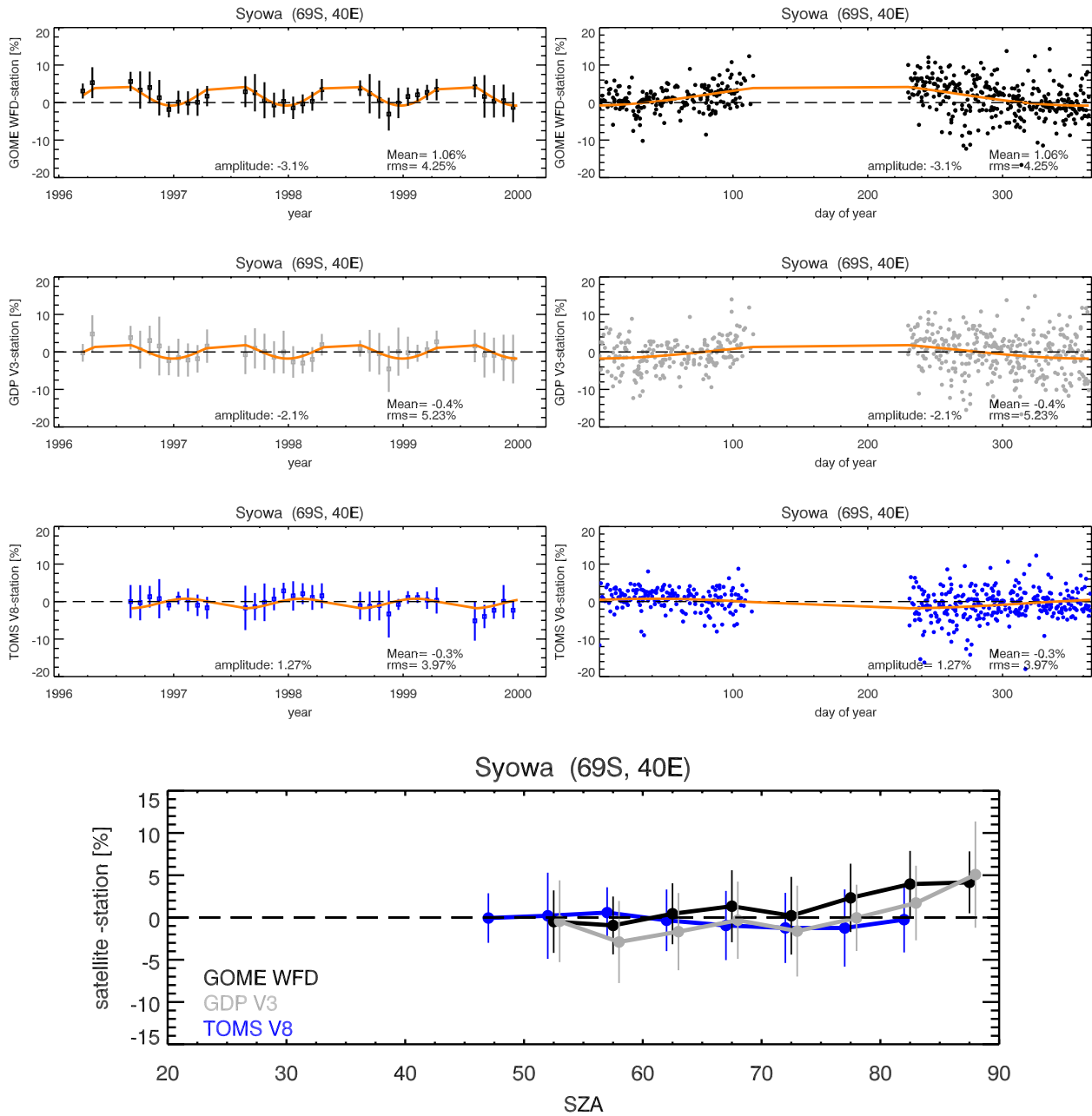


Figure 5.10: Same as Fig. 5.1 but for Syowa, Antarctica, 69°S.

Halley Bay, Antarctica, 74°S, Dobson

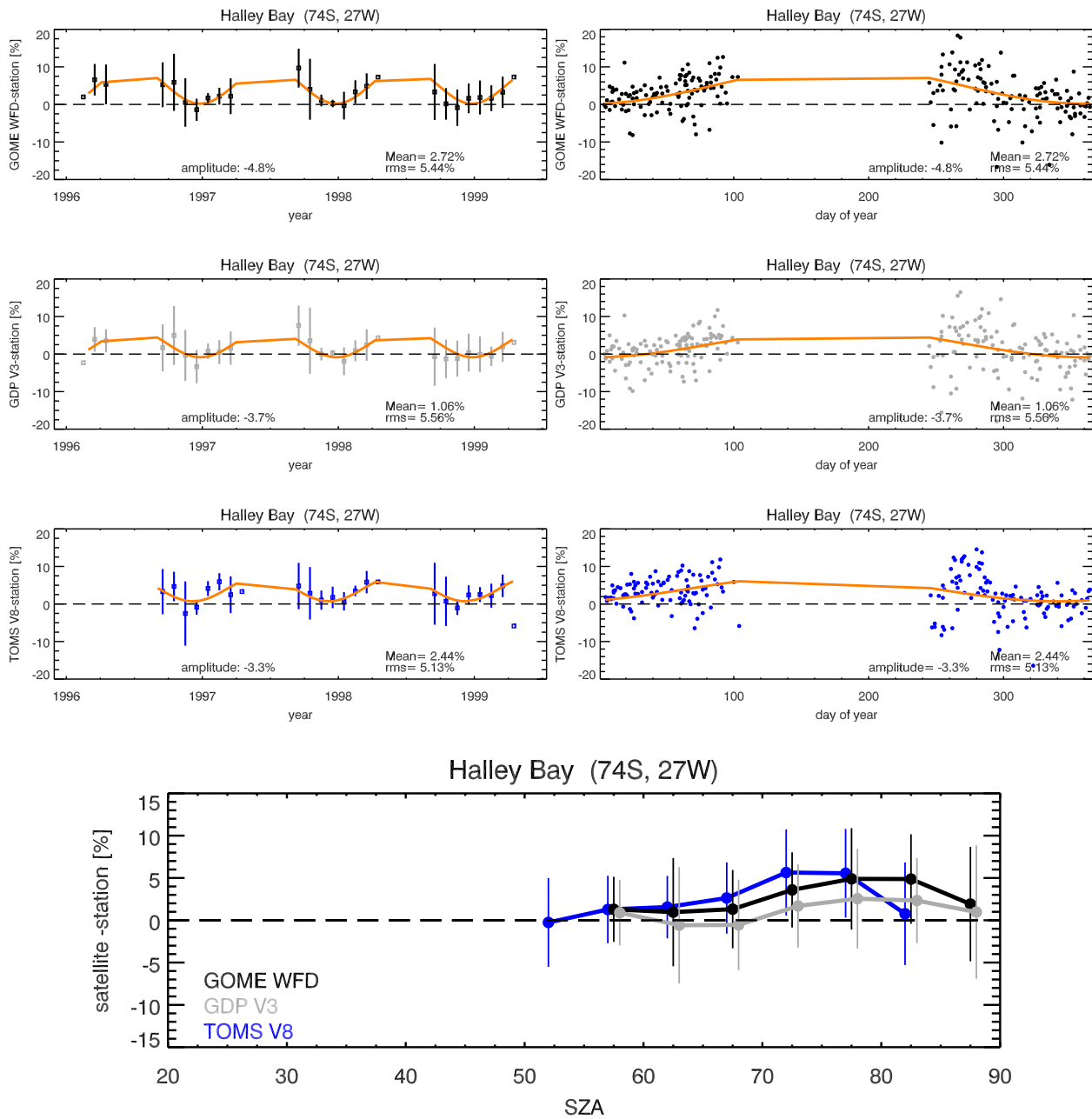


Figure 5.11: Same as Fig. 5.1 but for Halley Bay, Antarctica, 74°S.

6 Discussion

6.1 WFDOAS validation with ground station data

In this section the results from the comparison of satellite data (WFDOAS, GDP V3, and TOMS V8) with ground stations are summarised and discussed. The main results are:

- Ground stations at low and mid-latitudes
 - Excellent agreement between WFDOAS and ground stations with annual mean differences to within $\pm 1\%$. In general TOMS V8 mean differences are about 1% lower and GDP V3 differences about 2% lower than WFDOAS differences.
 - Seasonal cycle signature of WFDOAS differences show wave amplitudes of less than 0.5% and is even absent at some selected station e.g. Lauder. For comparison, the TOMS V8 seasonal amplitudes (w.r.t. ground) are on the order of 1% (up to 2% in case of Brewer measurements), while GDP V3 wave amplitudes are on the order of 1.5% to 2%. For all satellite data versions the wave amplitudes are generally higher for differences to SAOZ instruments than for the other instruments, Dobson and Brewer.
 - No significant solar zenith angle dependence is observed in the WFDOAS differences, while a trend is seen in the mid-latitude TOMS V8 differences (about -3% decrease for an increase of 60° in SZA). A possible explanation for the downward trend with SZA could be the neglect of the ozone profile shape dependence of the Ring effect in TOMS V8 (see Roozendaal et al. 2003).
- Polar region
 - In summer months agreement is to within $\pm 1\%$. This is very similar to the TOMS V8 differences while GDP V3 differences are generally about -2% with respect to the ground data. A clear exception in this case is Rothera, Antarctica, (UV/vis) where the differences are about +6% for WFDOAS and about +8% for GDP V3 and TOMS V8
 - Close to polar night period (at high SZA) WFDOAS differences increase to 2-5% on average. This is the case in fall (before ozone hole period) and spring (potentially ozone hole period dependent on hemisphere). Looking at the differences as a function of SZA a clear increase in the differences is observed beyond 70° SZA and reaches about +5% in the southern hemisphere. Such a tendency is not observed at Barrow, Alaska.
 - Under ozone hole condition the WFDOAS differences are generally 6% higher than TOMS V8 differences and about 3% higher than GDP V3 (all stations except Rothera). In general the latter are closer to the ground stations than WFDOAS. As discussed in the VALREPORT, the Dobson total ozone standard retrieval does not account for the ozone temperature (as done in WFDOAS) and comparison with Brewer measurements, where both ozone temperature corrections and careful stray light correction were accounted for in the retrieval, a difference of +3 to +4% was observed with respect to standard Dobson measurements (see Discussion on TOMS3-F campaign at Fairbanks in February and March 2001, in Staehelin et al., 2003). This is about the difference observed in the WFDOAS differences at high solar zenith angles.

6.2 WFDOAS Reference orbit comparison with TOMS V8

From Figs. 4.1 and 4.2 as well as Figs. A.1 and A.2 (Appendix A) the following results are obtained for the comparison of WFDOAS with TOMS V8:

- WFDOAS-TOMS V8 differences range from -2% to +1% for most months and latitudes
- A weak seasonal cycle signature is apparent in these differences with maximum in winter and minimum in summer at low and mid-latitudes.
- Differences are higher in the NH (ranging from -1% to +1%) than in the SH (-2% to 0%). The bias is largest at a GOME solar zenith angle of about 60° . A hemispheric bias is observed in the TOMS V7 version and it cannot be ruled out that some of that is still present, albeit to a lesser extent, in TOMS V8 (see Bramstedt et al., 2003). This hemispheric bias was not evident in the differences to the ground-based data (see above) for both WFDOAS and TOMSV8, but a downward trend in the ground-based TOMS V8 differences was found at mid-latitudes as a function of SZA that can contribute to this bias (larger solar zenith angles are more frequent the higher the latitudes).
- At very high solar zenith angles and in the polar region, the WFDOAS differences can reach +5% and higher particularly in SH polar spring. This is consistent with the validation results using ground-based data. The neglect of the ozone profile shape dependence of the Ring effect in TOMS V8 may contribute to differences of several percent between WFDOAS and TOMS V8.
- At specific times in the year and at specific locations large negative differences of -4% are observed, e.g. NH summer at 35°N and SH late fall at 60°S . At the lower latitudes this could point at differences in the treatment of aerosols. In WFDOAS the effective albedo acts as first order aerosol correction for non-absorbing aerosols, but an underestimation of a few percent is possible in the presence of absorbing aerosols as discussed in Section 3. From empirical relationships between aerosol index (derived from TOMS spectral data) and aerosol optical depth derived from collocated sun photometer measurements, a correction for absorbing aerosols has been introduced in the TOMS V8 retrieval and may explain part of these differences.

7 Inter-comparison of WFDOAS, TOGOMI, and GDOAS

This section contains the figures that compares all new GOME algorithms WFDOAS, GDOAS, and TOGOMI with each other and each of these algorithms with TOMS V8 based upon the reference orbits from 1997. Only the normal swath type data with 960 km across scan (East, Nadir, and West pixel) were used which was the case for 433 orbits out of 467. Figures 7.1 and 7.2 inter-compare the three algorithms among each other while Fig. 7.3 compares all GOME algorithms including GDP V3 with TOMS V8 in the manner as shown in Section 4. The solar zenith angle dependence of WFDOAS with the other GOME algorithms and TOMS V8 is depicted in Fig. 7.4. The 1σ scatter of the differences as a function of solar zenith angle have been calculated in a different manner as shown in Figs. 4.2 and A.2, where the scatter was determined from the individual GOME pixels. Here, the scatter was derived from the monthly mean differences that produces smaller RMS in the scatter.

We will leave the evaluation of the differences to the reader. One main conclusion can be drawn from this inter-comparison.

- All three GOME algorithms (WFDOAS, TOGOMI, and GDOAS) have converged reasonably well and all show larger systematic differences to GDP V3 and TOMS V8 than between each other.
- In the fine details some larger differences at specific conditions can be found between the new GOME algorithms, for instance, at high solar zenith angles in the polar region, that may be related to different approaches used in the algorithms.

In the following the major differences between WFDOAS and the other algorithms GDOAS and TOGOMI will be highlighted that may explain some of the features observed in the differences.

- All three algorithms account for the ozone absorption dependence of the Ring effect, but uses different ways to implement this. In WFDOAS full multiple scatter radiative transfer calculations are used to obtain the proper Ring spectra for different atmospheric scenarios parametrized by effective albedo, solar zenith angle, ozone climatology, and effective surface height. GDOAS and TOGOMI use approximations that do not require look-up tables like in WFDOAS. The good convergence of all three algorithms point at the validity of these approximations, but differences encountered particularly at very high solar zenith angles may indicate limitations of some of the approaches.
- WFDOAS uses the concept of effective altitude as derived from the cloud-top-height and cloud fraction retrieved with FRESCO (see Section 4.2 and Fig. 4.4 in ATBD). In addition for each GOME pixel the scene Lambertian Equivalent reflectivity is determined near 377 nm (see Section 4.3 in ATBD) and is used as effective scene albedo. This permits to a first order a correction for aerosol effects, particularly for non-absorbing types, and also takes into account sun glint effects. Using airmass factors like in GDOAS and TOGOMI the albedo for the clear-sky and cloud AMF remains fixed to a climatological value and 0.8, respectively.
- Other factors like spectral window selection, wavelength calibration (e.g. Fraunhofer fit), and polynomial degree selection (see Section 3) may contribute to differences between the three algorithms.

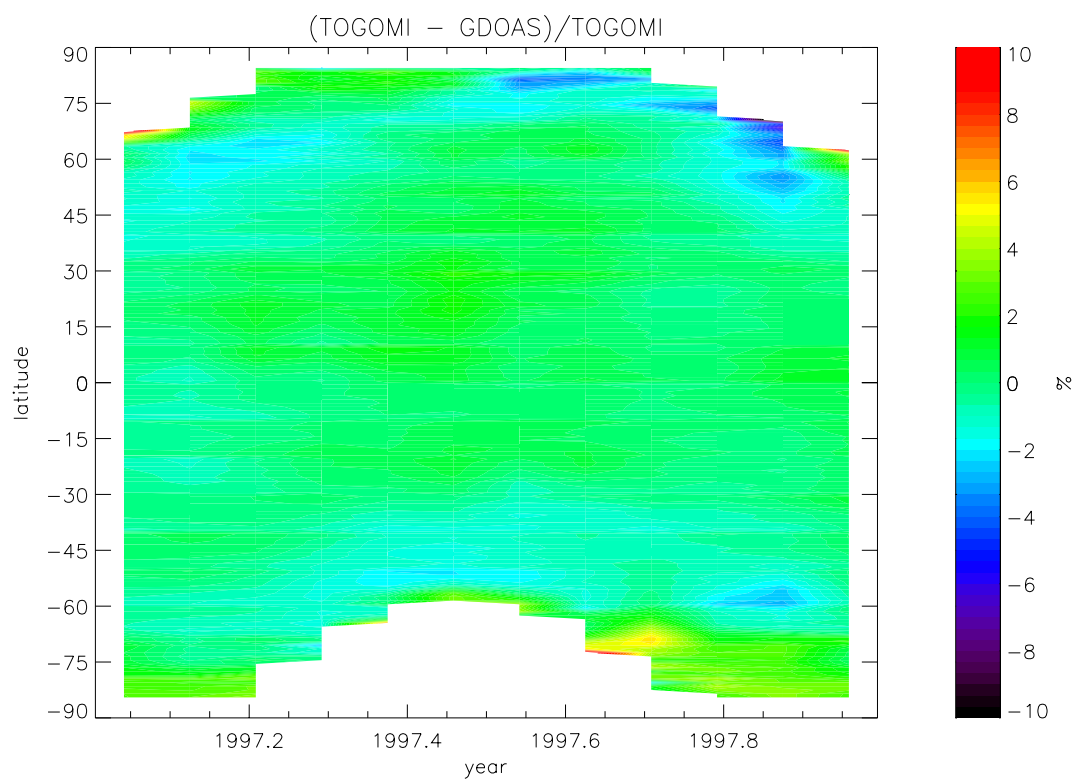


Figure 7.1: Monthly mean differences between *GDOAS* and *TOGOMI*.

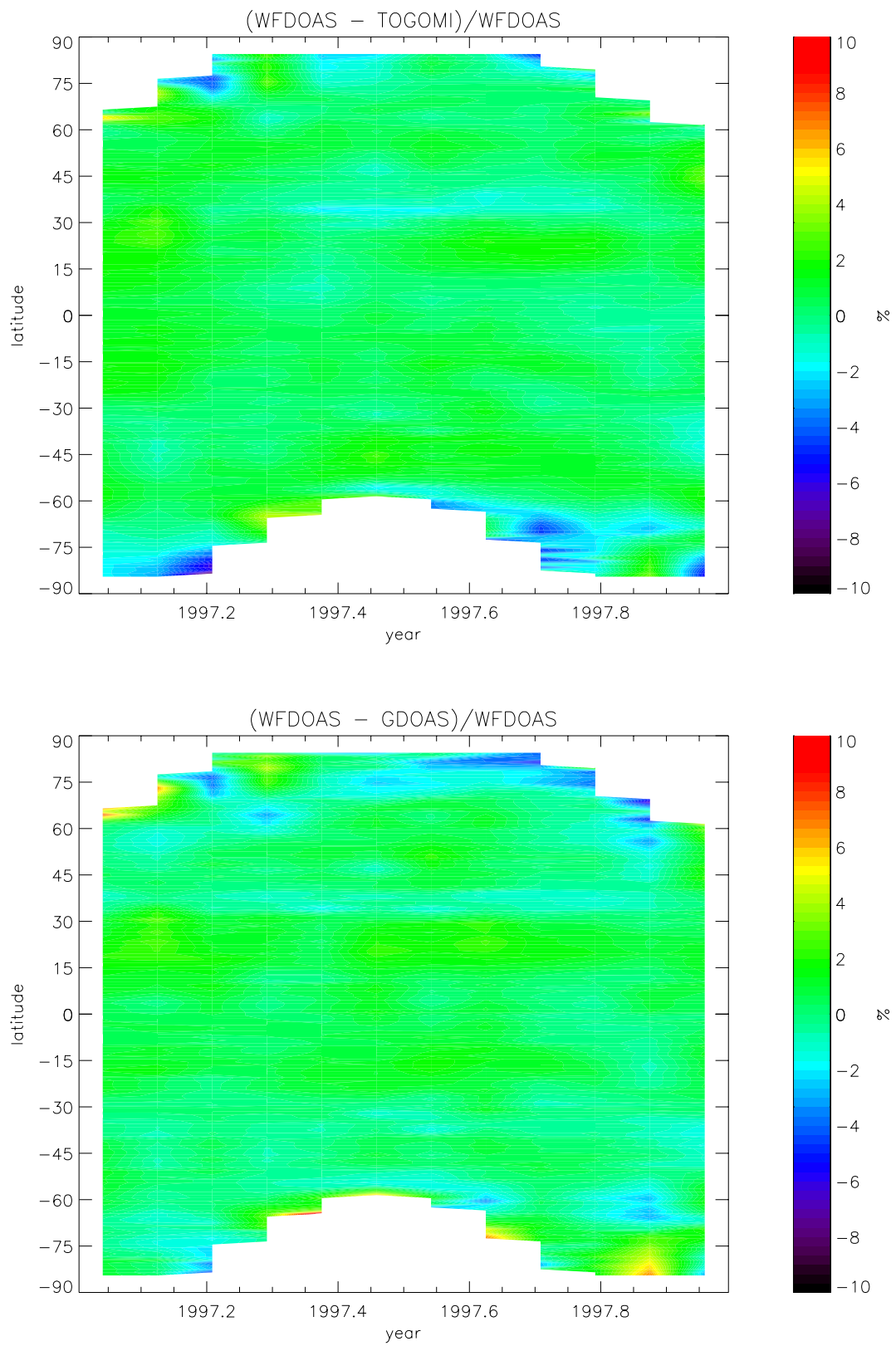


Figure 7.2: Monthly mean differences between WFDOAS and TOGOMI (top) and GDOAS (bottom).

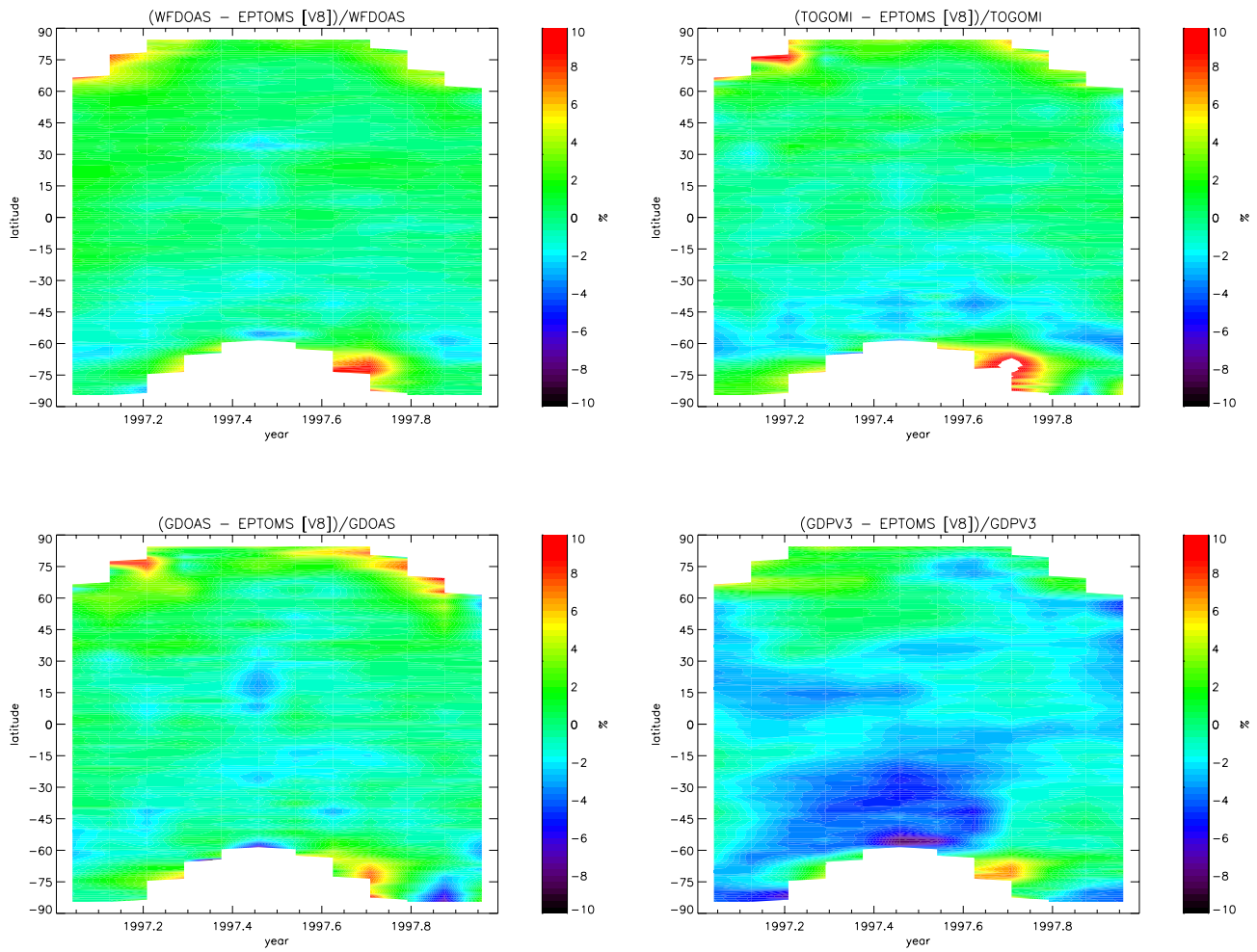


Figure 7.3: Monthly mean differences between GOME and TOMS V8: WFDOAS (top left), TOGOMI (top right), GDOAS (bottom left), and GDP V3 (bottom right).

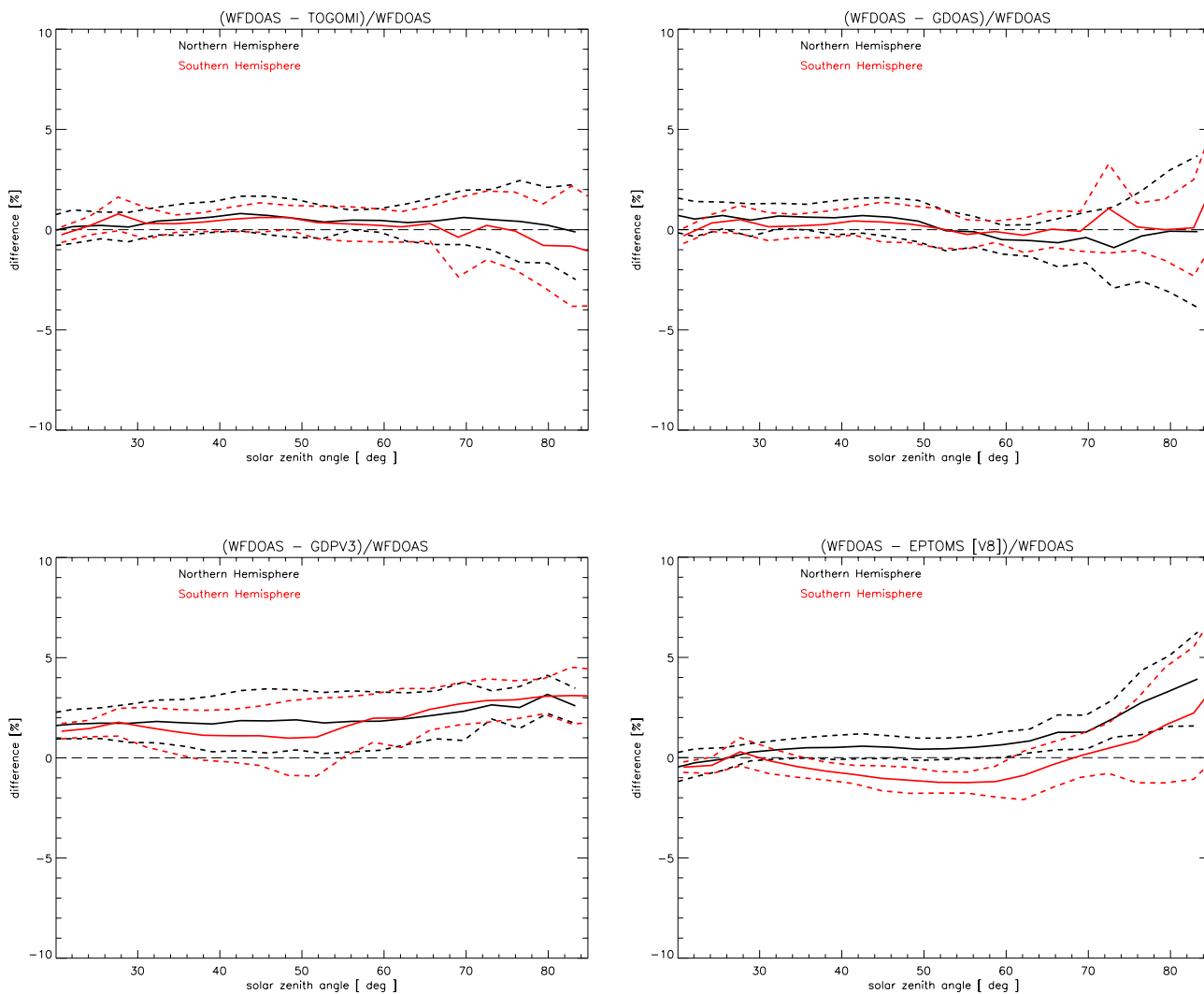


Figure 7.4: Solar zenith angle dependence of monthly mean differences between WFDOAS and TOGOMI (top left), GDOAS (top right), GDP V3 (bottom left) and TOMS V8 (bottom right). Dashed lines represents 1σ RMS of the monthly means.

8 Conclusion

The Delta Validation has confirmed the major findings from the VALREPORT with regard to the high quality of the WFDOAS GOME total ozone retrieval. The agreement of WFDOAS with collocated groundbased measurements show an annual mean bias that is to within $\pm 1\%$ and a seasonal cycle variation in the differences that have wave amplitudes well below 0.5% for most stations. In the polar region and at high solar zenith angles larger differences of up to +2 to +5% are observed. This range of values are within the uncertainty of ground-based instruments that in their standard retrieval (Dobson and Brewers) do not account for ozone temperature variation. Improved stray light corrections and accounting for ozone temperature in the ground-based retrieval will most likely increase ground-based values at high solar zenith angles (in fall/winter) by up to +3 to 4% (polar region) and +2 to 3% (mid-latitudes). From this one can conclude that the WFOOAS accuracy is well within the uncertainty of the ground-based instruments globally.

The comparison of GDP V3 with the same validation dataset together with the fact that the scatter of differences to ground data is much higher for GDP V3 are indication for the improved performance of WFDOAS over GDP V3. The inter-comparison between all new GOME algorithms (WFDOAS, TOGOMI, and GDOAS) has demonstrated that they have converged in their results and all represent a significant improvement over GDP V3. Some differences that still remain are most likely due to different implementations regarding ozone filling-in, albedo effects, and cloud correction schemes (effective height versus cloud airmass factors) despite the common use of FRESCO.

Appendix

A GOME Reference Orbit Comparison with TOMS V8 1996-2000

The reference orbit comparison as presented in Section 4 for 1997 has been extended to cover the period from 1996.5 to 2000.2. Results are summarized in the following figures and they basically confirm the findings in Section 4 as discussed in Section 6.

A.1 Contour plots for GOME-TOMS V8 differences

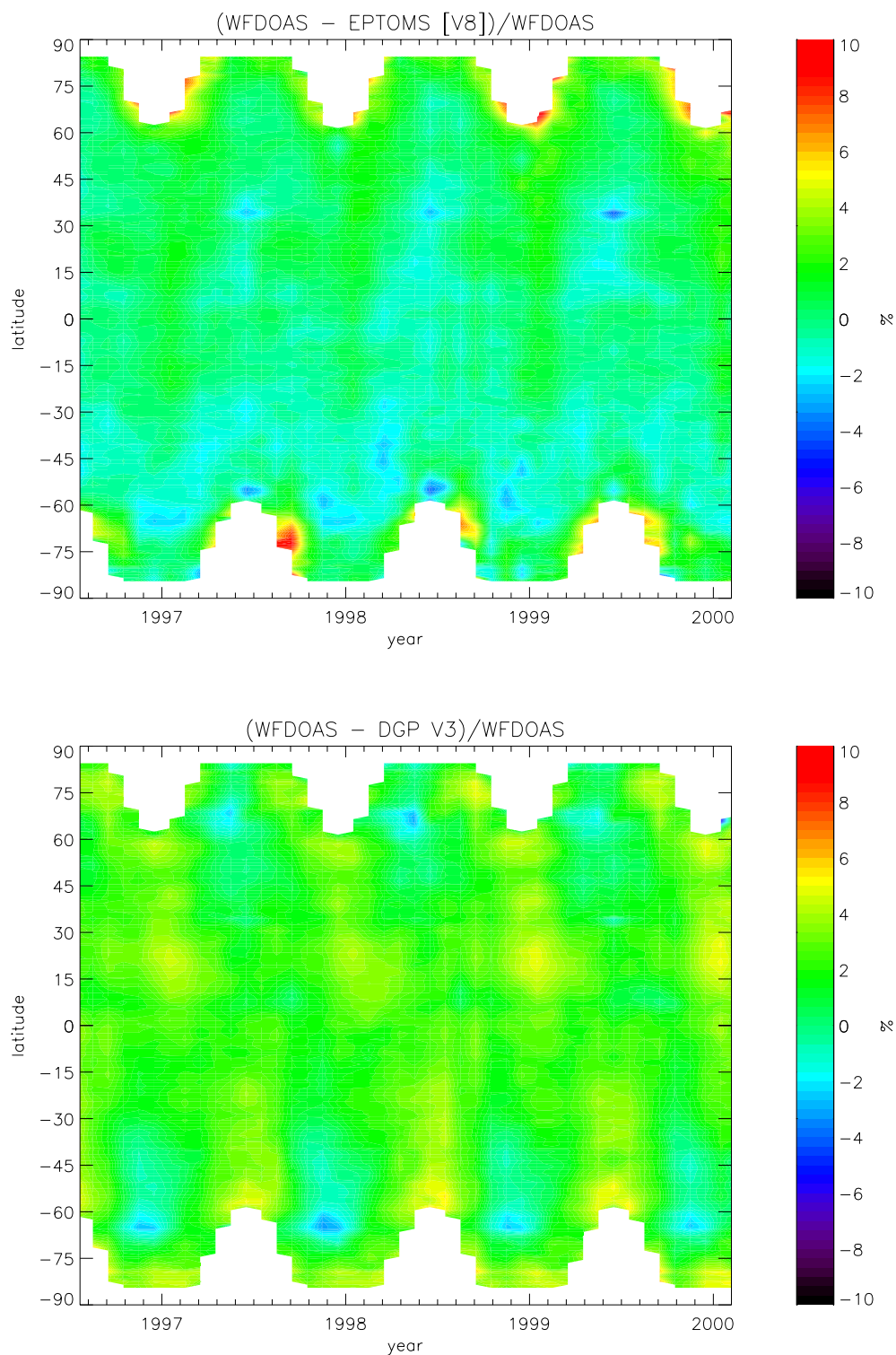


Figure A.1: Monthly mean differences between WFDOAS and daily gridded TOMS V8 data (top) and between WFDOAS and GDP V3 (bottom) for the GOME reference orbit dataset between 1996.5 and 2000.2.

A.2 Solar zenith angle dependence for GOME-TOMS V8 differences

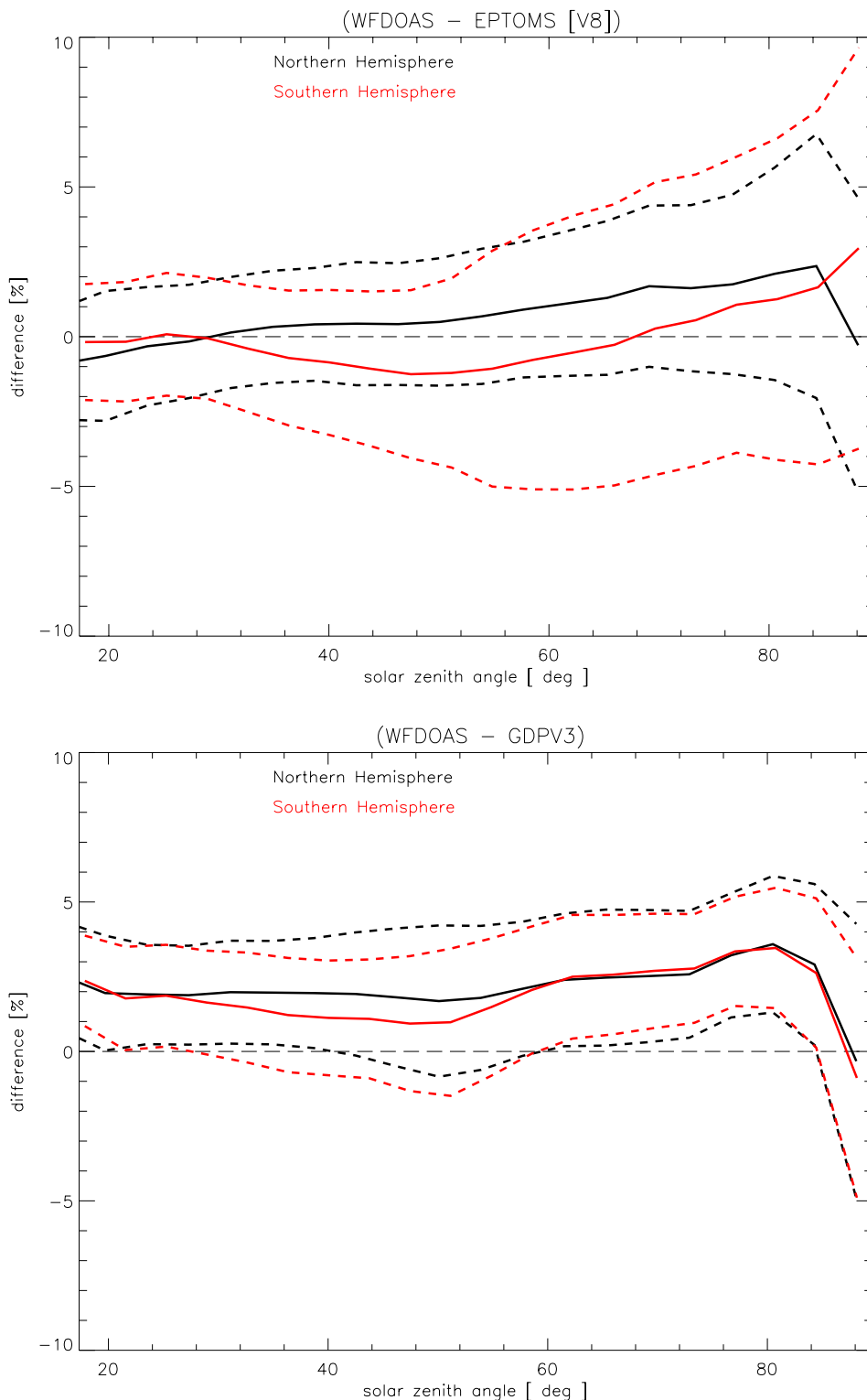


Figure A.2: Solar zenith angle dependence of the WFDOAS-TOMSV8 (top) and WFDOAS-GDPV3 (bottom) monthly differences as shown in Fig. A.1. Dashed lines are the 1σ RMS from binning all individual matches from the reference orbit data set.

B Cosine Fitting of Satellite-Station Difference Time Series

In many plots showing the time series of the differences between collocated satellite and station data a cosine with period of 366 days (seasonal variation) has been fitted to the daily differences as follows:

$$\Delta = A + B \cdot \cos[2\pi(t - \phi)].$$

Δ represents the dependent variable (satellite-station difference in percent) and t equals the day within a given year divided by 366. Fitting constants are A (annual mean), B (amplitude of wave), and ϕ (phase of wave). This non-linear equation (with respect to the fitting parameters) can be linearized by expanding the cosine as follows:

$$\Delta = A + B' \cos(2\pi \cdot t) + C' \sin(2\pi \cdot t),$$

with $B' = B \cdot \cos(2\pi \cdot \phi)$ and $C' = B \cdot \sin(2\pi \cdot \phi)$. B' and C' can be obtained from multivariate linear regression and are then solved for B and ϕ .

In Table 5.1 all stations that have been used in the Delta Validation are summarized. A summary of the fit results are presented in Table 5.2 and 5.3 for all stations and the various satellite data sets (WF-DOAS, GDP V3, and TOMS V8). It should be noted that for sparse time series like in high latitudes with an extended polar night period without data, the derived mean from the cosine fit may differ significantly from the annual mean derived directly from averaging the daily (or monthly) differences. For this reason the annual means are calculated and reported in two different ways.

C Plots with all Stations on one Page

In this Section the various presentation of the time series as plotted in Figs. 5.1-5.11 are regrouped such that all stations are here collected on one page.

C.1 Monthly mean difference time series for WFDOAS

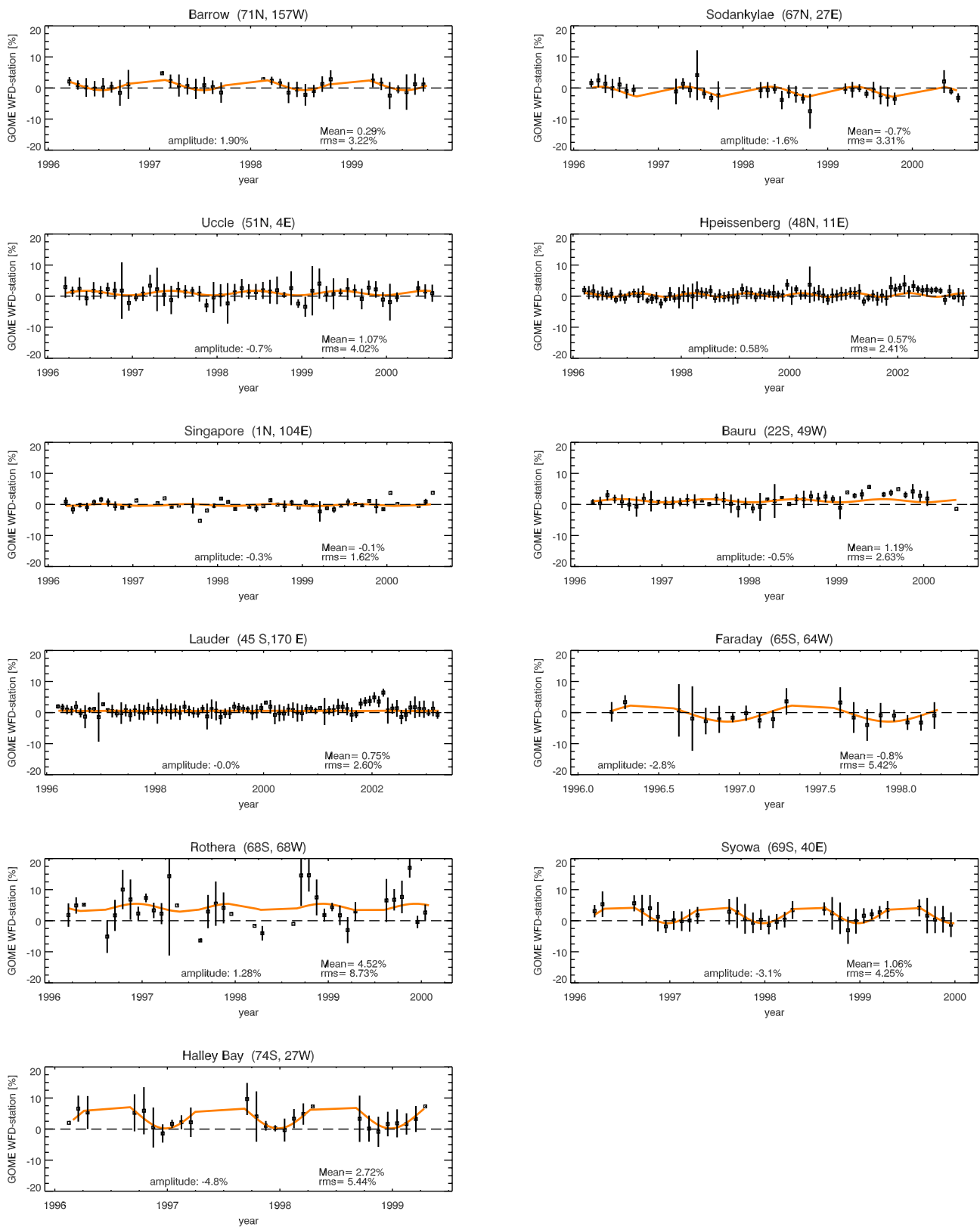


Figure C.1: Monthly mean time series of differences between WFDOAS and all ground-based stations

C.2 Monthly mean difference time series for GDP V3

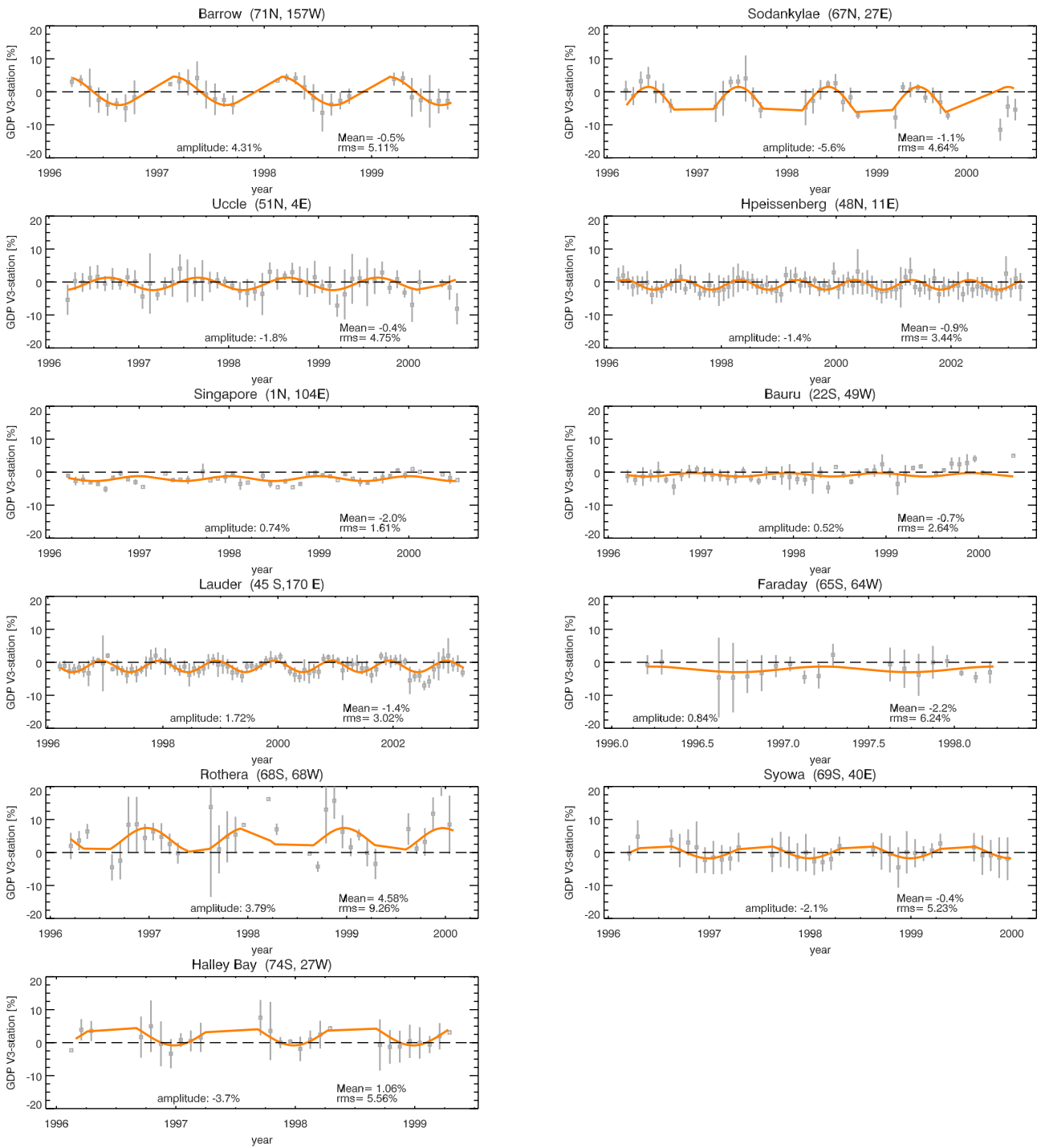


Figure C.2: Same as Fig. C.1 but for GDP V3.

C.3 Monthly mean difference time series for TOMS V8

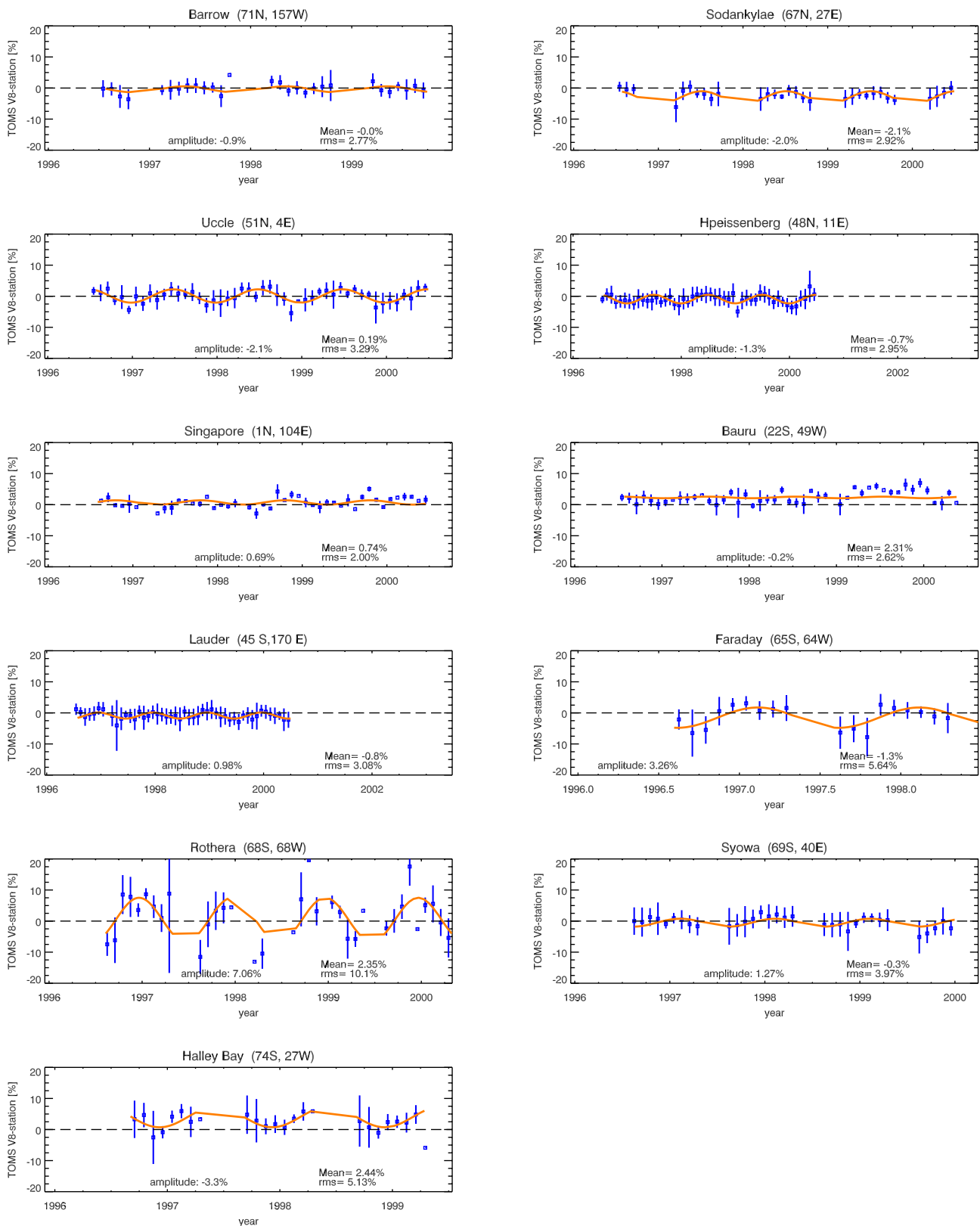


Figure C.3: Same as Fig. C.1 but for TOMS V8.

C.4 Annual course of daily differences for WFDOAS

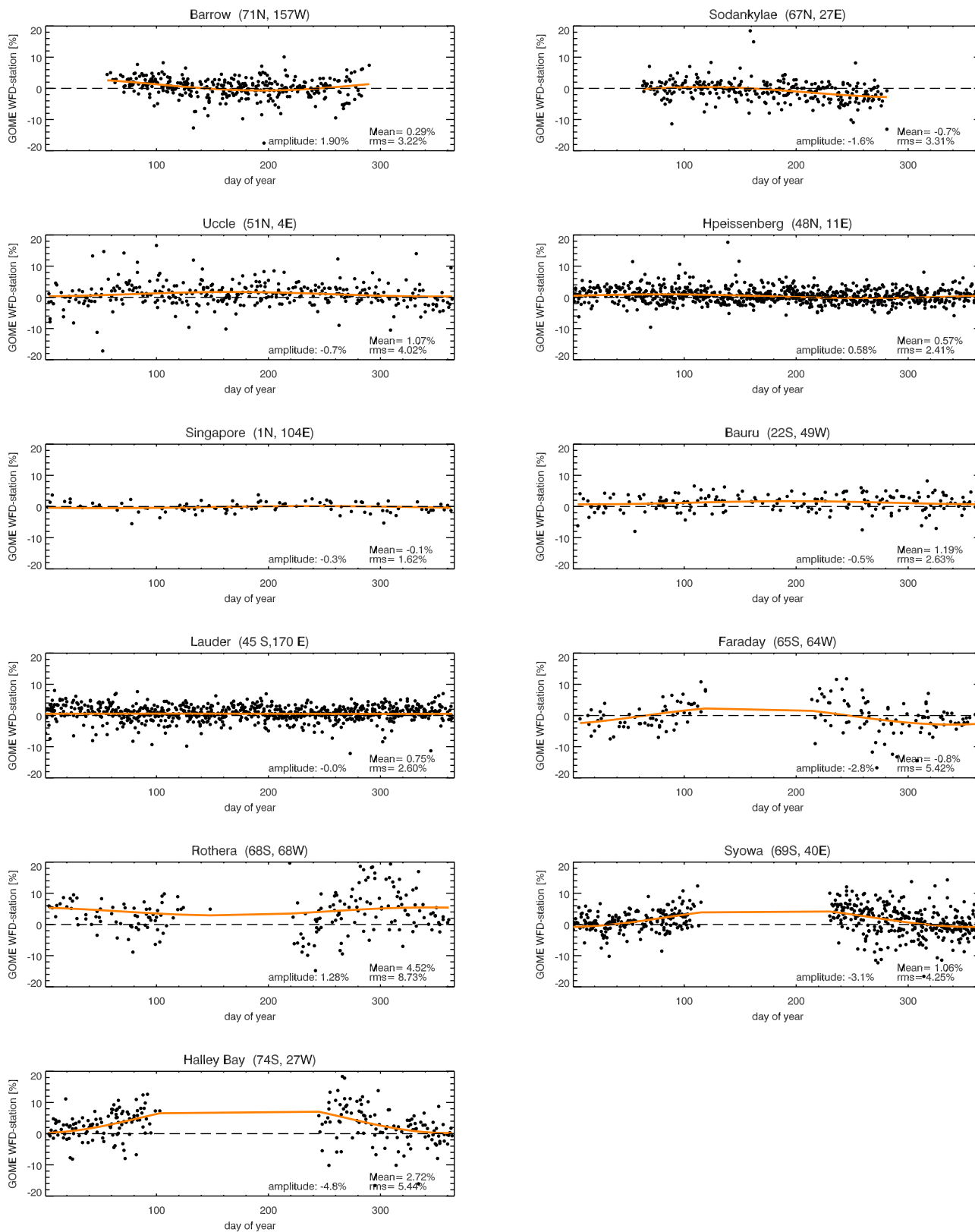


Figure C.4: Time series of daily differences between WFDOAS and ground-based data.

C.5 Annual course of daily differences for GDP V3

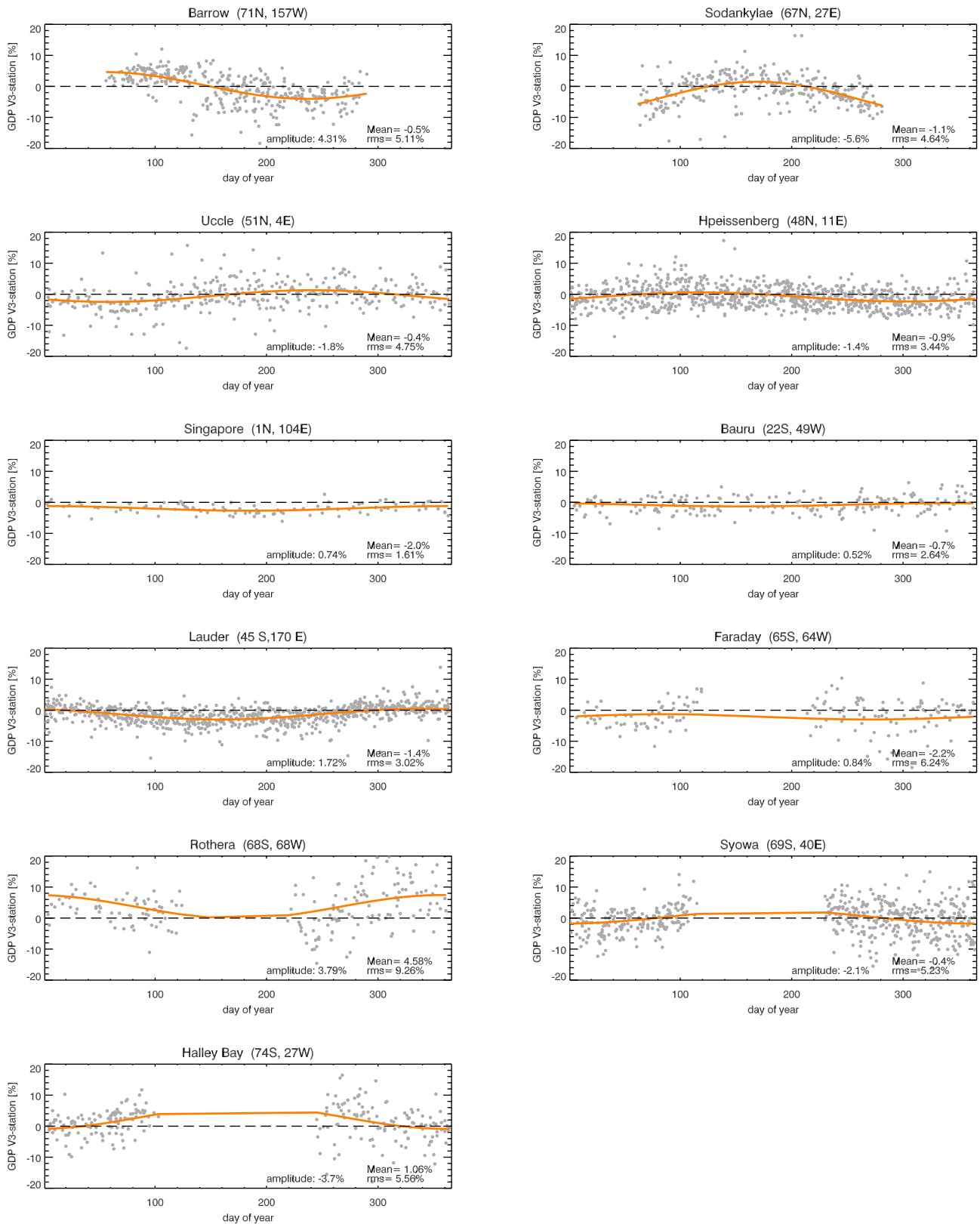


Figure C.5: Same as Fig. C.4 but for GDP V3.

C.6 Annual course of daily differences for TOMS V8

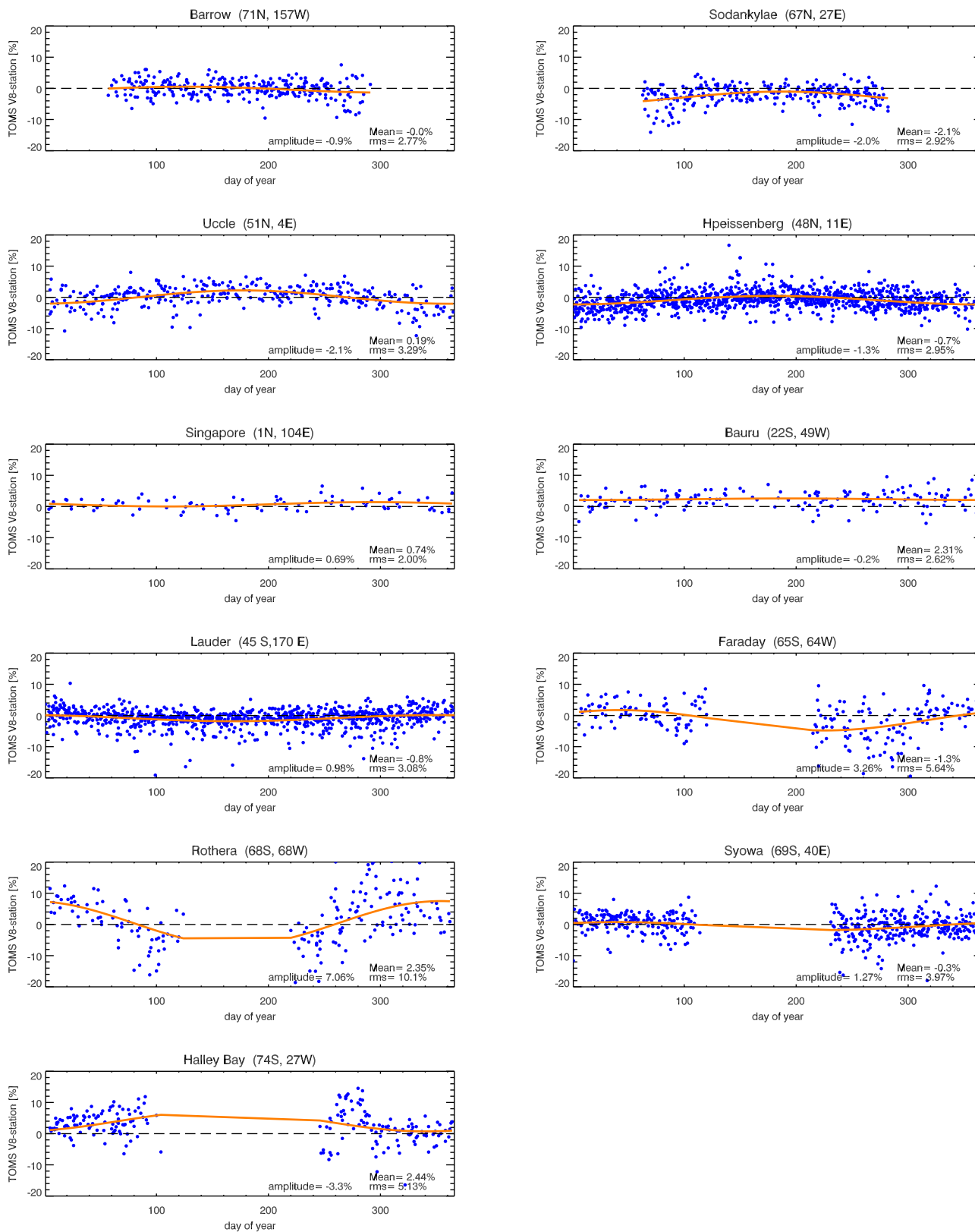


Figure C.6: Same as Fig. C.4 but for TOMS V8.

C.7 Solar zenith angle dependence for WFDOAS, GDP V3, and TOMS V8

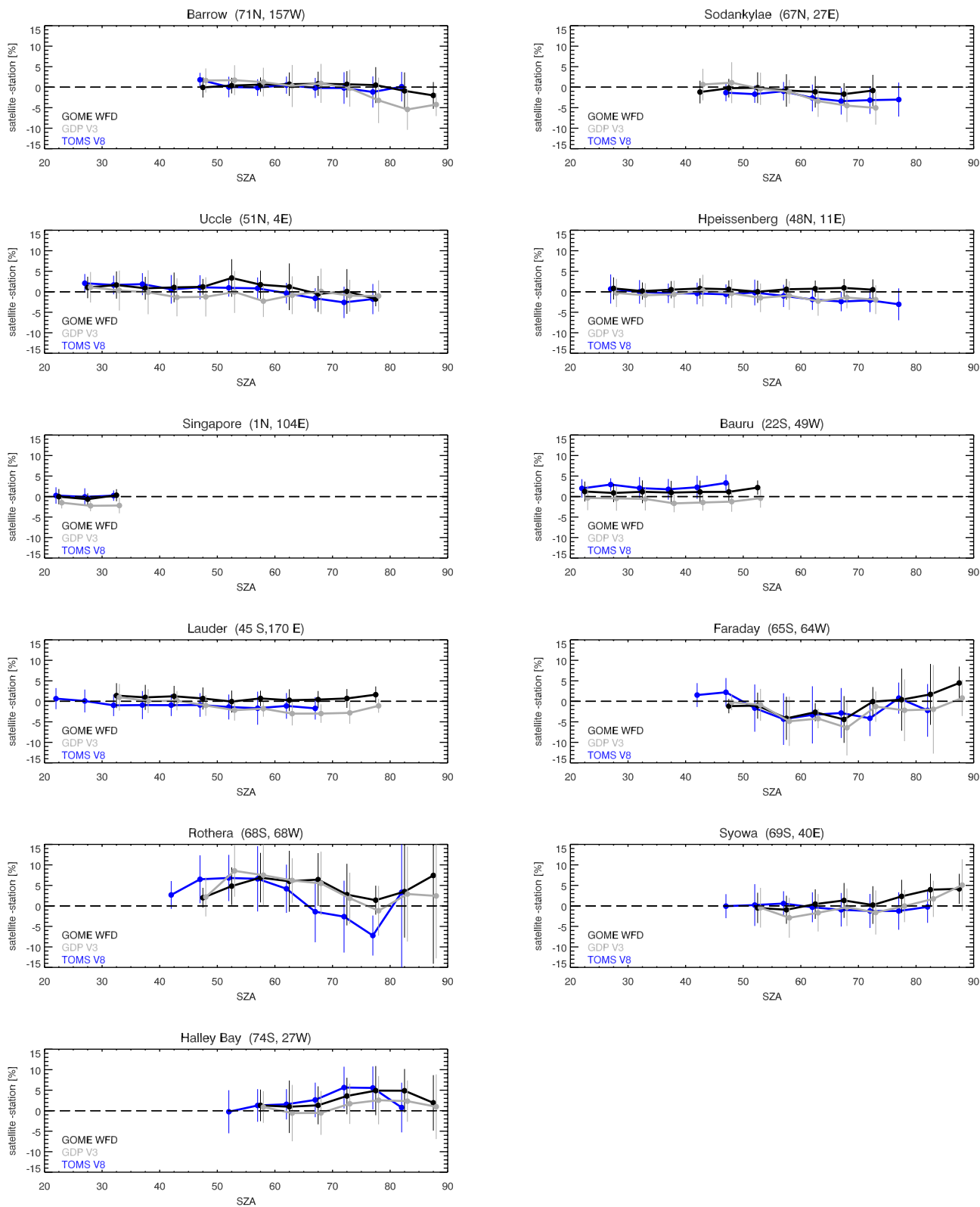


Figure C.7: Solar zenith angle dependence for satellite-station difference for WFDOAS (black), GDP V3 (grey), and TOMS V8 (blue).